Biol. Rev. (1995), **70**, *pp.* 67–106
Printed in Great Britain

FILTER-FEEDING IN MARINE MACRO-INVERTEBRATES: PUMP CHARACTERISTICS, MODELLING AND ENERGY COST

BY HANS ULRIK RIISGÅRD[1] AND POUL S. LARSEN[2]

[1] *Institute of Biology, Odense University, Campusvej* 55, *DK*-5230 *Odense M, Denmark*
[2] *Department of Fluid Mechanics, Technical University of Denmark, DK*-2800 *Lyngby, Denmark*

(*Received* 18 *October* 1993; *accepted* 14 *June* 1994)

CONTENTS

I. INTRODUCTION

(1) *Biology of filter-feeders*

Grazing on phytoplankton in marine macro-invertebrates implies feeding on highly dilute suspensions of food particles, too small to be sensed and seized individually. Suspension feeders must therefore process large volumes of water in highly efficient filters in order to meet their food requirements (Jørgensen, 1966, 1975). Typically, water processing is active, depending upon a pump to carry the water through the filter.

Suspension-feeding macro-invertebrates have evolved a variety of types of filter-pumps. But despite the great biological importance of the subject, the pumps and their properties were long a neglected field of research. Bidder (1923) made the first experimental and theoretical study of the fluid mechanics of a filter-pump on a calcareous sponge. With a delay of about 50 years. Reiswig (1975) extended the studies

to the demosponges. Chapman (1968) studied the hydraulic system of the filter-feeding echiuroid *Urechis caupo* and calculated the energy necessary for water pumping. Foster-Smith (1976*a*) determined the power required to sustain pumping rates in filter-feeding sponges, bivalves, polychaetes and tunicates, and he reviewed pump systems in tube-living animals (Foster-Smith, 1978). Vogel (1981) compiled and compared available data on the energy costs of pumping water, and Jørgensen (1983) reviewed the scattered and sparse literature on fluid mechanical aspects of filter-feeding. The design principles of fluid transport systems in, among others, suspension-feeding animals was examined by LaBarbera (1990), and Shimeta & Jumars (1991) reviewed the literature on mechanisms of particle capture by filter-feeders.

During the last decade, investigation of filter-pumps has, however, been intensified, including sponges (Riisgård *et al.*, 1993; Larsen & Riisgård, 1994), polychaetes (Riisgård, 1989; Riisgård & Ivarsson, 1990; Riisgård, 1991*a*; Riisgård *et al.*, 1992), bivalves (Jørgensen *et al.*, 1986*a*; Jørgensen & Riisgård, 1988; Jørgensen *et al.*, 1988; Jørgensen, 1989; Jørgensen, Larsen & Riisgård, 1990) and ascidians (Jørgensen *et al.*, 1984; Riisgård, 1988*a*). The studies have aimed at characterizing the pump systems quantitatively and assessing energy costs of water processing. This review of recent developments compares the different pump and filter systems and evaluates pump and filter capacities in an ecological context. As a corollary, some evolutionary trends are being suggested. As an introduction to the subject, a presentation is given of the basic principles of pump and system analysis along with the formulas used, and an approach to mathematical modelling of pumps.

(2) *Pump and filter system analysis*

Energy equation. Inspection of filter-feeding animals show that for each individual type, it is possible to identify a pump and a separate system of canals, filters, etc. which as a whole is called the system. The pump is a device that drives water at a certain flow rate against various resistances to flow present in the system.

The starting point for a simple analysis of a pump-channel system is the energy equation (the first law of thermodynamics). For steady, incompressible flow through a control volume from inlet state *in* to outlet state *ex* the energy equation, in the absence of heat transfer, may be expressed as (see Fox & McDonald, 1985, p. 160 and 260); or Garby & Larsen, 1994, p. 100)

$$[\Delta p_f + (p_{ex} - p_{in}) + \tfrac{1}{2}\rho(u_{ex}^2 - u_{in}^2) + \rho g(H_{ex} - H_{in})]\, Q = P. \tag{1}$$

Here, Δp_f denotes the frictional pressure drop and other resistances to flow through the system, p the static pressure, ρ the fluid density, u velocity, g acceleration of gravity, H the vertical height (or head), Q the volume flow rate, and P the power supply to the control volume. Equation (1) expresses that the sum of energies associated with resistance to flow and increases in pressure, kinetic and hydrostatic head equals the supplied energy, all per unit of time. For the particular case of no energy supply and for negligible resistance to flow, equation (1) reduces to the Bernoulli equation,

$$p + \tfrac{1}{2}\rho u^2 + \rho g H = \text{constant}, \tag{2}$$

which states that the sum of pressure, kinetic and potential energies is constant. This relation also shows that a pressure, or a pressure change, Δp, is conveniently expressed

as a change in hydrostatic pressure (or pressure head), $\Delta H = \Delta p/\rho g$, and a change in kinetic energy may be expressed as $\Delta H_k = (u_{ex}^2 - u_{in}^2)/2g$. Throughout, pressure heads, including $\Delta H_f = \Delta p_f/\rho g$, are used.

For filter-feeders, the inflow kinetic energy is normally zero since water enters as to a sink, having zero velocity far upstream. An exception would be an inhalant siphon facing an externally driven current. The exit flow, on the other hand, normally emerges as an organized jet flow whose kinetic energy cannot be neglected. Also, in their normal habitat, filter-feeders are surrounded by water, so $p+\rho gH$ is the same at inlet and outlet, irrespective of the orientation of the animal. An exception is the experimental condition of an imposed so-called back-pressure, $\Delta H_{12} = H_2 - H_1 = (p/\rho g + H)_{ex} - (p/\rho g + H)_{in}$, used to study the response of the pump-system of the animal to gain further information on the pump.

In view of the above remarks, equation (1) for the whole filter-feeder may be written as:

$$\rho g(\Delta H_f + \Delta H_k + \Delta H_{12})\, Q = P_p, \tag{3}$$

where P_p denotes the pump power received by the water flow and the sum of terms in the parenthesis is denoted the system head,

$$\Delta H_s = \Delta H_f + \Delta H_k + \Delta H_{12}. \tag{4}$$

Considering a control volume around the pump separately, and denoting the pressure rise from the inlet to the outlet of the pump by ΔH_p (the pump head), equation (1) for this control volume may be written as:

$$\rho g \Delta H_p\, Q = P_p. \tag{5}$$

From equations (3)–(5) follows:

$$\Delta H_p = \Delta H_s, \tag{6}$$

which simply states that the pressure rise delivered by the pump equals that required to maintain the flow through the system.

Characteristics. The steady state behaviour of the pump as well as the system, when either is studied separately, is described by the so-called pump as well as system characteristics which illustrate the changing pressure, ΔH, as a function of the volume flow rate, Q. As expected, most pumps will deliver a decreasing flow when forced to supply an increasing pressure rise, or pump head, ΔH_p, and the head loss of a system due to friction etc., ΔH_s, increases with increasing flow. When plotted on the same graph (Fig. 1*a*), the intersection of these two characteristics satisfies equation (6) and defines the operating point (O_{op}) of the pump-system arrangement in terms of the resulting operating flow, Q_{op}, and operating pressure head, ΔH_{op}, which can be read off the graph.

Pump characteristics. Typical pump characteristics are shown schematically in Fig. 1*b*. Open pumps with moving surfaces (ciliary lined walls of a canal, peristaltic motion of canal walls, free flagella or bundles of flagella) drive water flow through the action of viscous fluid forces (see, for example, Vogel, 1981). Such pumps invariably involve flows leaking back through the pump, a phenomenon which increases concurrently with higher pump pressure delivered. As a result these pumps have characteristics where flow decreases with increasing head. This is readily illustrated by the following simple

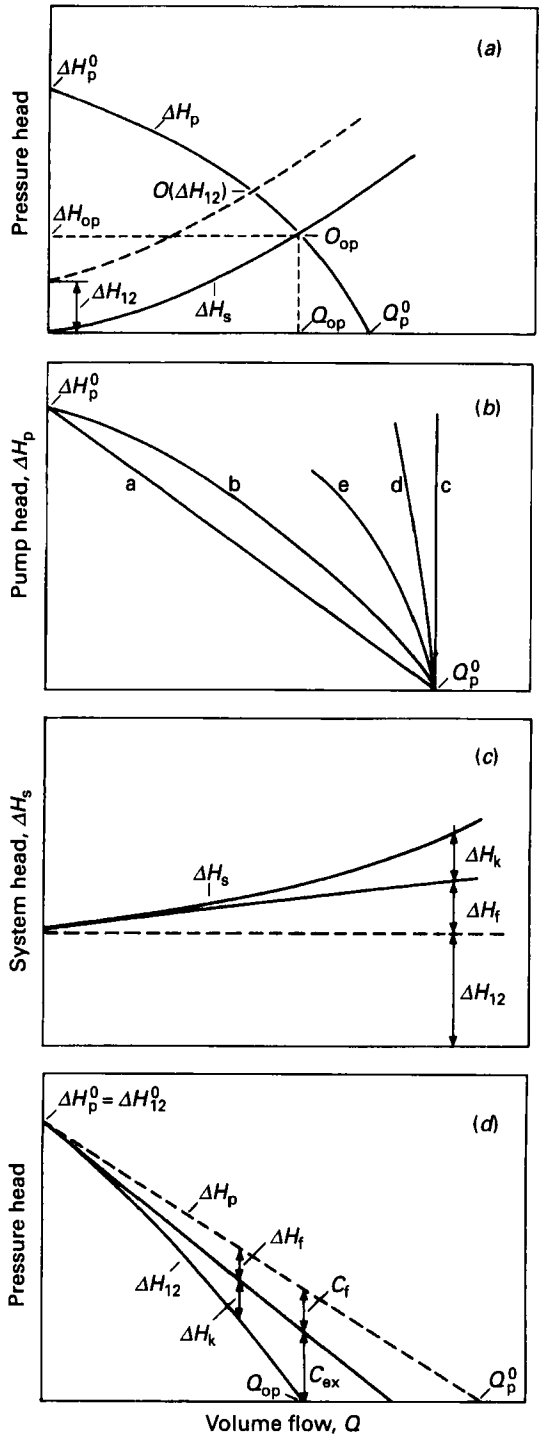

Fig. 1. (*a*) Pressure head plotted against volume flow, Q, to illustrate the pump characteristic (ΔH_p), i.e. the volume flow rate produced by a pump working against an increasing pressure head, and the system characteristic (ΔH_s), i.e. the pressure head needed to create different rates of flow in a given system. The point where the two characteristics intersect is termed the normal operating point (O_{op}), and the pressure head at this point is termed the normal operating pump pressure (ΔH_{op}). The corresponding volume flow

linear model. The net flow is the difference between the flow delivered by the moving surfaces, Q_p, and the leakage flow, Q_L,

$$Q = Q_p - Q_L. \tag{7}$$

Let $Q_p = Q_p^0$ (zero system resistance, see Fig. 1) be constant (true for streaming generated by a ciliary lined wall, for example, Nielsen & Larsen, 1993), and let the leakage be proportional to the pump head (true for many laminar viscous flows, see equations (15)–(21) below),

$$Q_p = Q_p^0, \quad Q_L = \text{constant } \Delta H_p. \tag{8}$$

Inserting equation (8) into equation (7), the result can be written as the linear characteristic (type (a) of Fig. 1*b*)

$$\Delta H_p = \Delta H_p^0(1 - Q/Q_p^0), \tag{9}$$

where the new constant, ΔH_p^0, is the maximum pressure head delivered by the pump at zero flow (shut-off head).

A closed pump (such as a piston pump, usually called a positive displacement pump) with perfect seals and hence without leakage, would ideally yield a constant volume flow (displacement volume multiplied by strokes per unit time) irrespective of the pressure rise delivered, see type (*c*) of Fig. 1*b*,

$$Q_p = A_p L_p f. \tag{10}$$

Here, the product of piston area and stroke length, $A_p L_p$, is the displacement volume and f is the stroke frequency. Any leakage associated with linear viscous flow, such as in equation (8), would give rise to a sloping linear characteristic (type (*d*) of Fig. 1*b*), subscribing to equation (9).

More complicated pump models arise if Q_p is not constant, or if Q_L is not simply proportional to ΔH_p. For example, if stroke frequency or stroke length in equation (10), and Q_L in equation (8) depend nonlinearly on ΔH_p (e.g. leakage flow associated with loss in kinetic energy, equation (23)), then a nonlinear (curved) pump characteristic arises (types (*b*) or (*e*) of Fig. 1*b*),

$$\Delta H_p = \Delta H_p^0 g(Q/Q_p^0), \tag{11}$$

where the nonlinear function g satisfies the relations $g(0) = 1$ and $g(1) = 0$. As suggested by Fig. 1*b*, pump characteristics always have negative slopes, with pump head decreasing with increasing flow, which is a necessary condition for stable operation of several pumps in parallel.

System characteristics. A typical system characteristic, ΔH_s versus Q (Fig. 1*c*), is the sum of three contributions, given by equation (4): a linear function of flow representing frictional resistance to flow,

$$\Delta H_f = C_f Q, \tag{12}$$

at Q_{op} is termed the normal operating flow (Q_{op}). The dashed line is an example of the system characteristic for a back pressure, ΔH_{12}. (*b*) Typical pump characteristics: (*a*) linear viscous pump, with linear leakage, (*b*) nonlinear viscous pump with leakage, (*c*) ideal positive displacement (piston) pump, (*d*) ideal positive displacement pump, with linear leakage, (*e*) ideal positive displacement pump, with nonlinear leakage. (*c*) Typical system characteristic, being the sum of contributions from an externally imposed back pressure, ΔH_{12}, a linear viscous friction, ΔH_f, and a quadratic kinetic head loss, ΔH_k. (*d*) Construction (schematic) of back-pressure characteristic ΔH_{12} (Q) from linear pump characteristic $\Delta H_p = \Delta H_p^0(1 - Q/Q_p^0)$, linear viscous head loss $\Delta H_f = C_f Q/Q_{op}$, and quadratic exit head loss $\Delta H_{ex} = C_k(Q/Q_{op})^2$.

a quadratic function of flow representing kinetic head loss,

$$\Delta H_k = C_k Q^2, \tag{13}$$

and a possible externally imposed back-pressure, ΔH_{12}, where C_f and C_k are constants. Equations for estimating ΔH_f and ΔH_k are more fully explained below.

Back-pressure characteristics. In addition to pump and system characteristics it is also important in experimental studies to define the back pressure characteristic of the animal. This is obtained by subjecting the entire animal to increasing levels of pressure at the exit (back pressure), ΔH_{12}, and measuring any subsequent change in the volume flow rate Q. Figure 1*a* shows the normal operating point O_{op} at zero back pressure ($\Delta H_{12} = 0$) as well as one operating point $O(\Delta H_{12})$ at a given back pressure. Figure 1*d* shows schematically the construction of the back pressure characteristic (ΔH_{12} versus Q) by the subtraction of two contributions to the system characteristic, linear friction (ΔH_f) and kinetic losses (ΔH_k), from the pump characteristic (ΔH_p versus Q). This corresponds to the substitution of equation (4) into equation (6) and solving for ΔH_{12}, and thus yielding the equation for the back pressure characteristic

$$\Delta H_{12} = \Delta H_p - \Delta H_f - \Delta H_k, \tag{14}$$

where ΔH_p is given by equation (9) or equation (11), and ΔH_f and ΔH_k by equations (12) and (13), respectively, all depending on volume flow rate Q.

System head losses. Following these general considerations we turn now to those factors which contribute to head losses in the system. Head losses may be due to apertures, frictional resistance in canals, annular spaces, pressure drop across lattices or nets, or kinetic head loss. Fig. 2 shows schematically the pressure head above that of the ambient fluid (the gauge pressure head) as it varies along the flow path of a pump and filter system due to different kinds of such resistances. At the normal operating point, at zero back pressure (case (*c*) of Fig. 2), the pressure head decreases along the inlet canal system due to frictional head loss, then increases over the pump, followed by a decrease along the exit canal system and an abrupt drop at the exit due to kinetic loss. The frictional and exit kinetic head losses become lesser as the flow rate is reduced due to increased back pressure (case (*b*) of Fig. 2), and they become zero as the flow rate becomes zero at a maximum back pressure (case (*a*) of Fig. 2).

Most flows in biological systems occur at low values of the Reynolds number, $Re = ud/\nu$, where d is a characteristic length, such as the diameter of the tube or an aperture, u is the mean velocity and ν the kinematic viscosity. Because of the low Reynolds number, the flow will be laminar and viscous forces will dominate over initia forces. For many such flows the frictional head loss will be linear with respect to both viscosity and velocity. This is particularly the case when $Re < 1$, which is referred to as creeping flow. These concepts of fluid flow, and many formulas for head losses, may be found in general textbooks (e.g. Marks, 1941; Leyton, 1975; Vogel, 1981; Fox & MacDonald, 1985). Nevertheless, to form a general view, we have compiled these formulas below using consistent symbols (defined at first appearance).

Apertures. The pressure drop for creeping flow with volume flow rate Q and mean velocity u through a circular aperture of diameter d can be calculated as (Happel & Brenner, 1965; p. 153)

$$\Delta H = 24Q\nu/gd^3 = 6\pi\nu u/gd. \tag{15}$$

Lattices and nets. The pressure drop across structures consisting of parallel circular

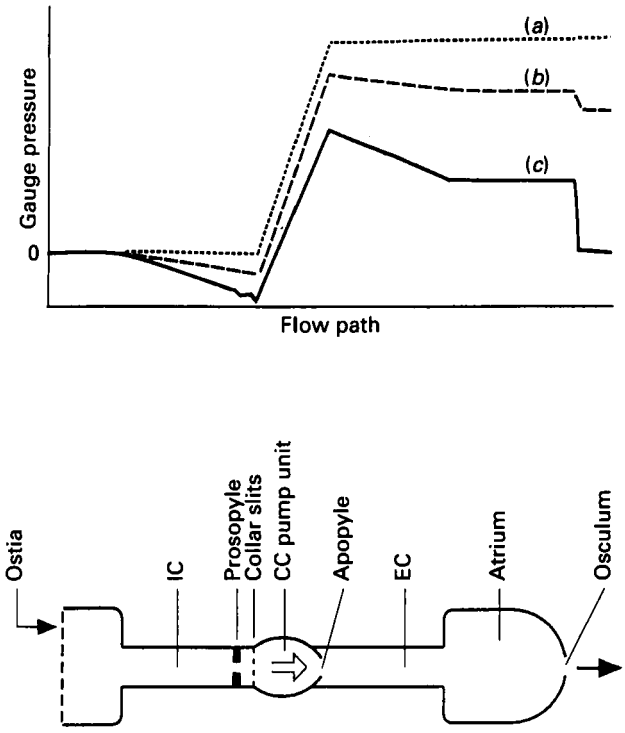

Fig. 2. Schematic pressure head variation along one flow path in a sponge, from ostia through inhalant canal (IC), prosopyle, collar slit, choanocyte chamber unit, apopyle, exhalant canal (EC) to atrium, with kinetic energy loss at osculum and at a back pressure of ΔH_{12}. (*a*) maximum back-pressure ($Q = 0$, $\Delta H_{12} = \Delta H_{12}^0$); (*b*) intermediate back pressure with reduced flow ($Q < Q_{op}$); (*c*) normal operating point ($Q = Q_{op}$, $\Delta H_{12} = 0$). (From Larsen & Riisgård, 1994).

cylinders with a diameter d spaced with a distance b between centres of neighbouring cylinders can be calculated from (Tamada & Fujikawa, 1957)

$$\Delta H = K_1 \nu u_\infty / g d, \tag{16}$$

where $K_1 = 8\tau/(1 - 2\ln\tau + \tau^2/6)$, $\tau = \pi d/b$, u_∞ = the mean velocity of the flow upstream of the structure. Silvester (1983) made a modification of equation (16) to the case of pressure drop across a uniform net of rectangular mesh built of cylindrical fibres

$$\Delta H = K_e \nu u_\infty / g h_e, \tag{17}$$

where $h_e = h_1 h_2/(h_1 + h_2)$; h_1 = width of mesh; h_2 = length of mesh; $K_e = 8\pi/(1 - 2\ln \tau_e + \tau_e^2/6)$; $\tau_e = \pi d/h_0$; $h_0 = h_1 h_2/\sqrt{(h_1^2 + h_2^2)}$; d = diameter of cylindrical fibre. A method of extending the use of equation (17) to nets of non-uniform meshes has been suggested by Riisgård *et al.* (1992). The pressure drop across square-mesh screens ($h_1 = h_2 = h$) at very low Reynolds number ($Re < 0{\cdot}1$) can also be estimated from the experimentally obtained formula of Munson (1988)

$$\Delta H = K_2 \nu u_\infty / g d, \tag{18}$$

where $K_2 = 4{\cdot}75(1 - \alpha^2)/2\alpha^2$, $\alpha = (1 - d/h)^2$. A comparison between equation (17) and equation (18) gives reasonable agreement for $d/h < 0{\cdot}1$.

Channels and ducts. For fully developed laminar flow in a tube (length = L; radius = r) the frictional head loss can be calculated as (Fox & McDonald, 1985; p. 360)

$$\Delta H = 8QvL/\pi r^4 g = 8vuL/gr^2. \tag{19}$$

For flow between coaxial cylinders (e.g. cylindrical core in a tube) the head loss can be calculated as (White, 1974; p. 124)

$$\begin{aligned}\Delta H &= [8QvL/\pi gR^4]\, n^4/[(n^4-1)-(n^2-1)^2/\ln n] \\ &= [8vuL/gR^2]\, n^2/[(n^2+1)-(n^2-1)/\ln n],\end{aligned} \tag{20}$$

where $n = R/r$ is the ratio of radii of tube and cylindrical core within the tube, and $Q = \pi r^2(n^2-1)u$. For flow between parallel plates, spaced a distance l apart, the head loss can be calculated as (Walshaw & Jobson, 1979; p. 183)

$$\Delta H = 12vuL/gl^2. \tag{21}$$

As flow enters a tube of diameter d from a plenum of much larger diameter, the flow becomes fully developed after a length of about $L_d \approx 0{\cdot}1\,d\,Re$. Clearly, this length can be ignored when $Re < 1$ so it is justified to consider fully developed flows in canal systems under these conditions. Exceptions to the above are typically found in siphons, say the inhalant and exhalant siphons of the mussel *Mytilus edulis* where $Re \approx 200$–300 and $L/d \approx 0{\cdot}3$–1 (Jørgensen *et al.*, 1986). Here, the flow never becomes fully developed and any loss due to friction along the walls of the siphon should be calculated from laminar boundary layer theory (White, 1974; p. 247). While this direct effect is usually negligible, there is an indirect effect in that the flow is retarded in the wall boundary layers which causes an additional acceleration of the core flow. Effectively, the flow area at the exit of the siphon of length L is reduced by the displacement thickness, $\delta_1 \approx 1{\cdot}72(vL/u)^{0{\cdot}5}$, around its perimeter. This area reduction should be taken into account when estimating the kinetic head loss at the exit.

Kinetic head loss. The velocity of water leaving a system through a constriction is estimated as u_{ex} = volume flow rate/area of opening. Since the kinetic energy associated with this flow is leaving the system and is therefore lost, there will be a contribution to the head loss that can be calculated as

$$\Delta H = u_{ex}^2/2g. \tag{22}$$

Minor losses. The frictional head loss associated with the inlet flow to a system and with area changes or constrictions within the system is traditionally expressed as

$$\Delta H = Ku_K^2/2g, \tag{23}$$

where u_K denotes the velocity of the smaller area and K is an empirical loss coefficient, see e.g. Fox & McDonald (1985) and Foster-Smith (1976*a*).

Pumping power. At any given operating point, the useful power received by the water is given by equation (5). At the normal operating point this becomes

$$P_{op} = \rho g \Delta H_{op} Q_{op}. \tag{24}$$

Energy expenditure. The aerobic metabolic power expenditure may be determined from the total respiration rate, R_{tot}, which can readily be measured in terms of the total oxygen consumption and which converts as $1{\cdot}0\ \mu l\ O_2\ h^{-1} = 5{\cdot}22\ \mu W$. It is often of

interest to relate the useful pumping power, P_{op} (i.e. the reversible power in the thermodynamic sense, which equals the minimum power of an ideal pump), to the metabolic power expenditure, R_{tot}. This ratio, the overall pump efficiency,

$$\eta = P_{op}/R_{tot}, \tag{25}$$

may be used to evaluate the energy cost of filter-feeding.

Approach to modelling. To determine the pump power requires both volume flow and pump head at normal conditions, equation (24). As explained below, the volume flow may often be measured with little difficulty. However, the pump head cannot be measured directly, mainly because the pump is often an integral part of the whole flow system and cannot be isolated. Therefore, an indirect approach is needed. One way is to measure the back-pressure characteristic, ΔH_{12} as function of Q (see below), and then derive expressions for ΔH_f and ΔH_k as function of Q using standard equations for head losses, such as equations (15)–(23), and detailed morphological data on the geometry of the flow system. This amounts to a theoretical estimate of the system characteristic, hence the pump characteristic is determined from equation (14) and the pumping power at the normal operating point from equation (24). To justify these results it remains to characterize the pump and to verify, through separate modelling, that the pump design and function may in fact perform as predicted.

Temperature effects. One way to verify the models is to study the effects of changes in temperature on pumping rates. Bivalves in Danish waters, for example, are seasonally acclimatized to function normally from temperatures as low as 2 °C in February to 21 °C in June (Jørgensen, 1990). As expected, observed pumping rates decrease with decreasing temperature, which may be a result of separate physical and biological effects.

The dominant physical effect is the increase in kinematic viscosity with decreasing temperature (e.g. by a factor of 1·6 from 25 °C to 5 °C for 35‰ salinity, according to Rawson & Tupper, 1968). For the system, this causes a proportionate increase in viscous resistance to flow, equation (15)–(21), provided the geometry and linear dimensions of flow channels, nets, apertures, etc. remain unchanged. Even minor contractions of the diameter of a channel or aperture would give additional significant increases in viscous resistance.

For open pumps, the leakage flow, Q_L in equation (7), if associated with viscous resistance, would be of the form

$$Q_L = \text{constant } \Delta H_p/\nu, \tag{26}$$

and the driven flow, Q_p, if driven by a moving surface of specified streaming velocity (e.g. a ciliated surface with beat frequency f), would be of the form

$$Q_p = \text{constant } f. \tag{27}$$

Combining equations (26) and (27), the result may be written as

$$\Delta H_p = \Delta H_p^0(\nu/\nu^0)\,[(f/f^0) - Q/Q_p^0], \tag{28}$$

where ν^0 and f^0 are reference values of kinematic viscosity and beat frequency, respectively.

As another model, suppose the driven flow, Q_p in equation (7), were a result of a constant force delivered by a moving wall (cilia). From the definition of viscosity, the

shear force at the wall is proportional to viscosity and velocity gradient or, for developed laminar flow, the mean velocity or the volume flow rate, hence equation (27) would be replaced by

$$Q_p = \text{constant } \nu^{-1}. \tag{29}$$

Using this result, and retaining equation (26) for the leakage flow, equation (28) would then be replaced by

$$\Delta H_p = \Delta H_p^0[1-(\nu/\nu^0)(Q/Q_p^0)]. \tag{30}$$

The dominant biological temperature effect is the exponential increase in metabolic activity with increasing temperature, usually modelled by the Q_{10}-factor, defined as

$$Q_{10} = (R_2R_1)^{10/(T_2-T_1)}, \tag{31}$$

where R_1 and R_2 are the metabolic rates at two temperatures T_1 and T_2. This general equation permits the calculation of Q_{10} (i.e. increase in rate due to 10 °C increase) when observations have been made at two temperatures that are not 10 °C apart. Q_{10} for metabolic rate is usually between 2 and 3 for biological processes. Thus, Q_{10} for pumping rate may be used to evaluate if temperature effects on pumping rate are due to expected changes in rates of biological processes or partly due to physical effects. If Q_{10} for pumping rate is higher than 2–3 this indicates that physical effects are also making an impact. Beside changes in viscosity the physical effects may be exerted e.g. through changes in morphological dimensions of pump and flow system.

(3) *Experimental methods*

The empirical counterpart of the above-mentioned analyses is the experimental determination of geometric configurations and dimensions, volume flow rate, pressure and pressure differences, and fluid properties of biological pump systems.

The density and kinematic viscosity changes of seawater as a function of salinity and temperature are well known (Rawson & Tupper, 1968). Seawater is a Newtonian fluid (as has been assumed in the flow analysis in the previous section) and its viscosity is not affected by the presence of food particles in the concentrations normally encountered. This is readily verified by the expression for the first order approximation to the effective kinematic viscosity for dilute suspensions $\nu_s = \nu(1+5\Phi/2)$ (e.g. Happel & Brenner, 1965), where Φ denotes the volume of the particles as a fraction of the whole. However, there may remain some questions as to the validity of the equations given above when the diameter of a channel or an aperture approaches that of the food particles. If the particle concentration is low however, the periodic increase in pressure drop may contribute little to the average pressure drop.

The geometry and dimensions of flow systems are usually assumed to be well established from morphological studies of filter-feeders using optical and electron microscopy. It is recognized, however, that these techniques are often intrusive and hence have associated errors. As a result, the theoretical predictions of pressure drop, assuming that the flow rate is known, may only be approximate. This is evident, for example, for a given flow through a tube where equation (15) indicates the pressure drop to be inverse proportional to the fourth power of radius. Also, the degree of disturbance of the filtering animal may change the flow geometry, say the valve gape and consequently the distance between gill filaments and opening of exhalant siphon

(Jørgensen, 1990). Suboptimal conditions and/or mechanical disturbances may yield results that differ considerably from those from an undisturbed and optimally pumping individual. Such experimental aspects are beyond the scope of this paper, however, and only a brief presentation of experimental methods for measuring flow and pressure will be given.

(*a*) *Volume flow rate and back-pressure characteristics*

During the last 60–70 years many attempts have been made to determine the volume flow rate (also called the pumping rate or the filtration rate) of suspension feeding bivalves and other macro-invertebrates (Jørgensen, 1966, 1975, 1990). There are many measurements of pumping rates in the literature, especially for bivalves, but the results are often difficult to compare due to the different techniques employed. The methods used are traditionally grouped into two categories, (1) direct methods where the exhaled water flow is collected and measured ('constant-level tank', e.g. Famme, Riisgård & Jørgensen, 1986) and (2) indirect methods where the pumping rate is inferred from either the rate of change in concentration of suspended particles ('clearance method', e.g. Coughlan, 1969; Riisgård, 1977; Møhlenberg & Riisgård, 1979), or from a representative velocity measured in the exhalant flow ('thermistor probe', e.g. LaBarbera & Vogel, 1976; Foster-Smith, 1976*b*; Meyhöfer, 1985).

The direct method using a constant level tank was devised by Galtsoff (1926) and later improved by Famme *et al.* (1986) to give reliable data in agreement with those from the 'clearance method'. A version of the apparatus is shown in Fig. 11*a* where the inhalant and exhalant currents of the experimental animal are physically separated by a silicone rubber membrane so that the water being pumped from the inhalant chamber (C_1) is collected in the exhalant chamber (C_2). The increasing water level in the exhalant chamber (C_2) is monitored with a laser beam striking a mirror fixed on a floating ping-pong ball. The mirror reflects the laser beam onto a scale situated 8–10 m from the mirror, and a deflection of 1 cm on the scale corresponds to about 0·1 mm change in water level in C_2. When the animal pumps water from C_1 to C_2, a pressure difference develops which may be fixed at any selected value by adjusting a calibrated peristaltic pump that pumps water back from C_2 to C_1. By means of this method both the volume flow rate at zero back pressure (Q_{op}) and the back pressure characteristic can be determined experimentally (Figs 7*a*, 11*b* and 13). The use of this method is limited however, to animals which have a well defined exhalant siphon (such as e.g. *Mytilus edulis* and *Styela clava*) or osculum (e.g. *Haliclona urceolus*), or to animals which pump water through a tube in which they are living (e.g. *Nereis diversicolor*, *Chaetopterus variopedatus*). When using such a direct method, great care must be taken to avoid mechanical disturbance of the animal. Such mechanical errors do not apply to the use of the indirect clearance method, where the volume flow rate is measured as the volume of water cleared of suspended particles in unit time. The reduction in the number of particles as a function of time is followed by taking water samples at fixed time intervals and measuring the particle concentration, usually with an electronic particle counter. Clearance (Q_c) is determined from the exponential reduction in algal cell concentration as a function of time using the formula

$$Q_c = (V/Nt)\ln(C_0/C_t), \tag{32}$$

where C_0 and C_t are the algal concentration at time o and time t respectively, V = volume of water and N = number of experimental animals. If the suspended particles are 100% efficiently retained by the filter system of the animal then $Q_c = Q_{op}$. By recording particle size distributions as a function of time, a class of large particles that are fully retained can usually be identified, and this will yield the total flow rate. The ratio of flow rates determined from the depletion of the smaller particles to the total flow rate then gives the retention efficiency of different sized particles (e.g. Møhlenberg & Riisgård, 1978; Riisgård, 1988*b*).

Indirect methods based on the measurement of velocity of exhalant streams by a small thermistor probe (LaBarbera & Vogel, 1976; Vogel, 1981; Meyhöfer, 1985) requires accurate positioning, temperature control and probe calibration. The sensing element in a thermistor (as in a hot-wire or hot-film) is a small resistor that is heated to a temperature above that of the surrounding fluid by passing an electrical current through it. The cooling of the element depends on the local flow velocity past it, hence the electric power, or the resistance which depends on its temperature, becomes a measure of velocity. In principle, the complete velocity distribution over the full flow area, say of an aperture, should be recorded to give the volume flow. In practice, however, a single velocity measurement may give the desired result provided the probe has been calibrated in a flow from an aperture of identical geometry and having an identical velocity distribution (see Foster-Smith, 1976*b*).

Local velocities can alternatively be deduced from particle tracking, observed visually through a microscope or recorded on video with subsequent image analysis (Nielsen *et al.*, 1993).

The main reasons for the wide discrepancies between authors using different indirect methods have been pointed out by Riisgård & Møhlenberg (1979) and Møhlenberg & Riisgård (1979). It has been shown that the different indirect methods agree well when used properly under comparable experimental conditions. The 'clearance method' has proved to be especially reliable and is frequently used as a method for measuring both volume flow rate and particle retention efficiency.

(*b*) *Pressure and pressure drop*

Ideally, it would be desirable to measure the hydrostatic pressure at various positions along a flow system through a filter-feeding animal. This would allow a check of modelling, it would give volume flow rate if the geometry were known precisely, and it would allow a direct study of the pump characteristic if the pump itself could be clearly defined. There are several reasons why this is difficult. Pressure differences are often small and access is intrusive and may therefore change the fluid mechanics and the animal's state. According to engineering standards, static pressure in a channel with any significant velocity should be measured through pressure taps at the channel wall, i.e. through a small hole ending flush with the inside wall of the channel. If the velocity within the canal is negligible, however, any probe terminating within the chamber may be used.

Chapman (1968) recorded the external pump pressure in the tube of the filter-feeding echiuroid *Urechis caupo* by connecting a manometer to a hole in the tube containing the animal. Peak pressures during peristalsis were used along with independent measurements of flow rates to estimate pumping power. Foster-Smith (1976*a*) used a

sensitive pressure transducer cell ending in a hypodermic needle probe, implanted and sealed through a hole drilled in the shell of bivalves, to record pressures in the mantle and suprabranchial chamber. He also manufactured a fine glass tube with a proper static pressure hole drilled into its side just behind the sealed tip. The probe was inserted through the apertures of inhalant and exhalant siphons to directly measure pressure gradients of flow along these siphons. Jones & Allen (1986) using a similar method found pressure differences for the mantle and suprabranchial chamber that were much larger than those of Foster-Smith. This suggests the difficulties in performing such experiments. It is important to note that the frictional pressure drop between coaxial cylinders (assuming the probe to be centred in the siphon) may be sizably greater than in an undisturbed tube, and that corrections should be made. This can be seen from the ratio of equations (20) and (19). For example, assuming the same volume flow and a diameter ratio of $n = 6$, the measured pressure gradient would be more than twice that prevailing without the probe.

II. SPONGES

(1) *Functional morphology: filter mechanism and pump design*

Sponges are sedentary, filter-feeding metazoans whose body is specialized for suspension feeding. The basic principles for water pumping and particle retention are the same in all sponges. In general, water enters the body of the sponge through numerous small openings (ostia) on the surface (Fig. 3*a*). Water then flows through a branched inhalant canal system to the water pumping units, the choanocyte chambers (Fig. 3*b*), within which there are numerous choanocytes each with a beating flagellum and a collar-filter (Fig. 3*c*). These filters efficiently retain small suspended particles, including free living bacteria, and colloidal organic matter (Reiswig, 1975; Frost, 1978; Bergquist, 1978; Jørgensen, 1983; Simpson, 1984) and the filtered water leaves the choanocyte chamber through an opening to the exhalant canals which merge into one or more openings or oscula on the surface (Fig. 3*a*).

The structure of the choanocytes is the same in all sponges and among the metazoa, sponges are unique in feeding by means of choanocytes. Choanocytes are structurally and functionally identical to choanoflagellates which are a group of flagellate protozoans that filter free-living bacteria in the sea (Fjerdingstad, 1961*a*, *b*; Laval, 1971; Hibberd, 1975). Larsen & Riisgård (1994) analysed the sponge pump and compared it with the choanoflagellate pump in order to identify prerequisite properties of the basic pump unit which has enabled the evolution of large sponges with long inhalant and exhalant canal systems. These long canal systems in turn give rise to considerable frictional resistance to water flow (Riisgård *et al.*, 1993).

The comparative pump analysis made by Larsen & Riisgård (1994) was based on experimentally measured back-pressure pumping-rate characteristics of the demosponge *Haliclona urceolus* combined with mathematical-hydraulic modelling. The maximal pressure rise delivered by *H. urceolus* (at zero flow) was experimentally measured to be *c.* 2·7 mm H_2O. To determine the pumping principle for sponges, a free-living choanoflagellate (*Monosiga*) was considered as representative of a sponge choanocyte because the two cell types are structurally and functionally identical. In both systems, a flagellum pumps water through a collar of microvilli which acts as a filter. Knowing the flagellum length, beat frequency, wavelength and amplitude the

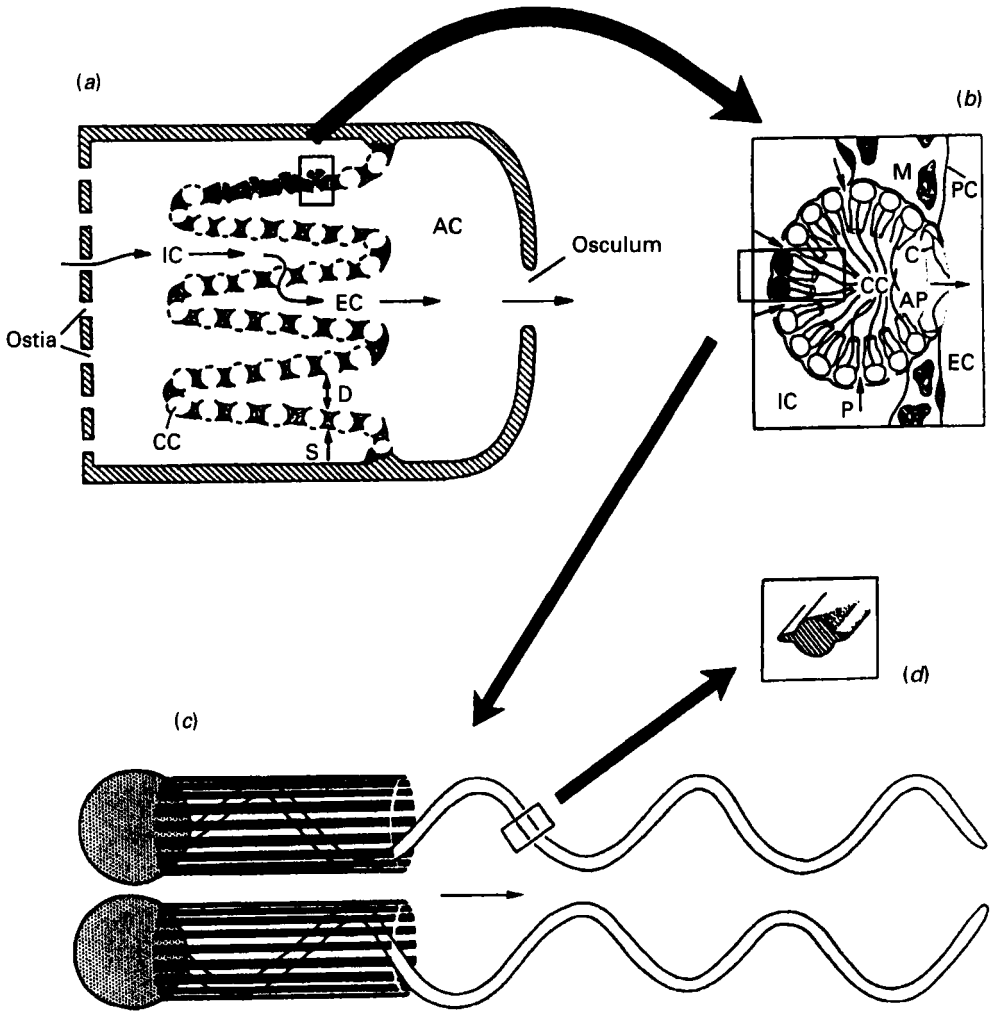

Fig. 3. (*a*) Schematic outline of advanced sponge design (leucon-type) with tapered inhalant (IC) and exhalant (EC) canal system (diameter *D*), separated by walls (thickness *s*) with embedded single-stage basic pump units (CC) in parallel and same pressure rise ΔH_p and flow Q_{cc}. (*b*) Choanocyte chamber (CC) separating inhalant canals (IC) and exhalant canals (EC), arrows indicate the direction of water flow through the prosopyles (P) into the CC and exit through the apopyle (AP) surrounded by a cone cell (C). The CC is immersed in mesohyl (M) encircled by pinacocyte cells (PC); (*c*) Two choanocytes with parallel flagella acting as a peristaltic pump. (*d*) Cross section of flagellum showing projecting ridges. (Adapted from Larsen & Riisgård, 1994).

pump head of the choanoflagellate was estimated to be 0·08 mm H_2O. Because this pump head was considered as insufficient to lead to the pressure drop measured in a sponge, it was suggested that the closely spaced flagella in the choanocyte chambers of sponges, possibly confined as a bundle by the apopyle, might together act as a peristaltic pump capable of creating the necessary pump pressure to overcome the resistance of the extensive canal system. This theory was supported by calculations based on characteristics of two-dimensional peristaltic pumps from the literature which showed that a sufficient order of magnitude of pressure rise could be achieved in this way. It was

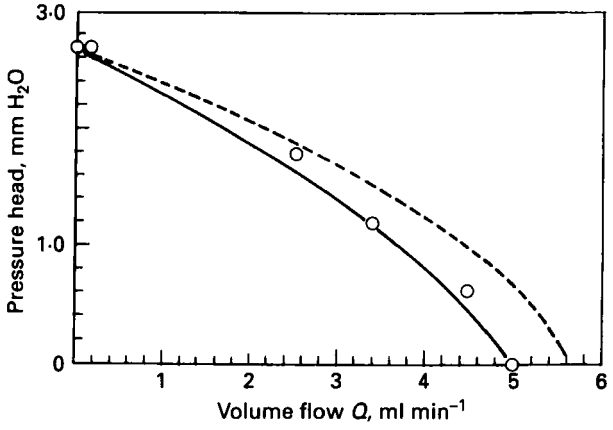

Fig. 4. Modelled nonlinear pump characteristic of sponge pump (dashed line) and resulting back pressure characteristic (solid line). Experimentally determined values (open symbols) for *Haliclona urceolus* are shown for comparison. (From Larsen & Riisgård, 1994).

concluded by Larsen & Riisgård (1994) that the basic pump units in demosponges are the choanocyte chambers and not the individual flagella.

(2) *Energy cost and pump model*

The uniformity of the basic anatomic structure of demosponges (Reiswig, 1975) and the near identical filtration rates recorded for *Halichondria panicea* and *Haliclona urceolus* prompted Riisgård *et al.* (1993) to define a 'standard sponge' (dry weight = 0·1 g) with a maximal filtration rate of 6 ml min^{-1} and a respiration rate of 15 μl O_2 h^{-1} at 12 °C. The shape and dimensions of the 'standard sponge' were as follows: shape = tubular/cylindrical: 32 mm long, outer diameter = 8·6 mm, diameter of atrium = 2·3 mm, diameter of osculum = 1·5 mm. The other dimensions of the aquiferous system were based on *Haliclona permollis* derived from Reiswig (1975).

To determine the normal pump pressure of the 'standard sponge pump' and subsequently to calculate the pump power output, the sum of head losses along the flow path through the canal and filter system of the sponge (i.e. the system characteristic) was calculated by Riisgård *et al.* (1993). To allow for such calculations, it was necessary to make some assumptions about the anatomy of the sponge, including the length, diameters of canals and chambers etc., and about the flow velocity in the different regions along the flow path. The aquiferous canal system in the 'standard sponge' was described as follows: Water enters the sponge through numerous ostia (mean diameter = 20·6 μm) on the surface and passes through a quickly branching system of narrow inhalant canals (IC) of 300, 100 and 50 μm diameter, respectively, similar to that of the stem system of a tree and then to the choanocyte chambers (CC; diameter = 30 μm), which were considered as the basic pump units. All pump units were assumed to operate in parallel at the same flow and working pressure, the density of CCs was estimated to be 12000 mm^{-3} and the CCs were estimated to constitute 30–50 % of the wall structure separating inhalant and exhalant canals. Within each CC there were assumed to be 60–100 choanacytes (Fig. 3*c*), each with a beating flagellum (Fig. 3*d*).

Water enters the CCs through an inhalant opening (prosopyle) with a diameter of 1–5 μm. The beating flagellum draws water through a 'collar-filter' surrounding each flagellum. The collar consists of a circular row of approximately 5 μm long and 0·14 μm diameter fibrils with a slit of 0·11 μm between adjacent fibrils (i.e. the centre distance between fibrils = 0·25 μm). Water flows from the CCs through the exhalant opening (apopyle; diameter = 14 μm) which is surrounded by a ring of cone cells into a system of exhalant canals (EC), which mirrors the inhalant system. Finally, the water channels of all exhalant systems merge into the atrial cavity (Fig. 3*a*) which has an exit osculum (diameter = 1·5 mm) on the surface through which the filtered water leaves the sponge as a strong jet.

The head loss along the flow path and the energy cost of pumping in the 'standard sponge' was estimated by Riisgård *et al.* (1993), as summarized below.

Inhalant and exhalant canals. Assuming a constant pressure gradient along the inhalant canals and by calculating this pressure gradient, the total frictional pressure drop in a 3 mm long IC of the 'standard sponge' was found to be 0·121 mm H_2O. Because this pressure reduction also applies for the EC's the total head loss along both the inhalant and exhalant canals was calculated to be 0·242 mm H_2O.

Apertures. The pressure drop for creeping flow with known volume flow and mean velocity through the circular apertures of ostia and prosopyles with known diameters was calculated by means of equation (15) as 0·037 and 0·115 mm H_2O for ostia and prosopyles, respectively.

Collar slits. Assuming that all flow passes through the 0·11 μm wide slits between the collar fibrils (diameter, $d = 0{\cdot}14$ μm), spaced at a distance, $b = 0{\cdot}25$ μm, between centres of neighbouring fibril-cylinders, then equation (16) calculates the pressure drop over the collar-filter to be 0·122 mm H_2O.

Exit loss. Knowing the area of osculum (0·018 cm^2) and the pumping rate (6 ml min^{-1}) of the 'standard sponge', the velocity of water leaving the osculum was estimated to $u_{ex} = 55{\cdot}6$ mm s^{-1}. Using equation (22) this exit velocity suggests a contribution of 0·158 mm H_2O to the total pressure reduction.

Pumping power. Adding all the above calculated contributions, the total system pressure drop, which in turn defines the normal operating point is $\Delta H_{op} = 0{\cdot}242 + 0{\cdot}037 + 0{\cdot}115 + 0{\cdot}158 = 0{\cdot}673$ mm H_2O. The power output could then be calculated from equation (24), yielding $P_{op} = 0{\cdot}677$ μW. With a respiration rate $R_{tot} =$ 15 μl O_2 h^{-1}, equivalent to 80 μW, the overall pump efficiency, equation (25), was found to be $\eta = P_{op}/R_{tot} = (0{\cdot}677/80)100 = 0{\cdot}85\,\%$.

Pump characteristic and modelling. Figure 4 (open symbols) shows an example of back pressure-pumping rate characteristics measured for *Haliclona urceolus*. The maximal pressure rise which could be delivered by the sponge pump (at zero flow) was about 2·7 mm H_2O. Assuming the validity of the measured back-pressure characteristic and the computed system characteristic it was clear that the pump characteristic could not be of the linear form of equation (9). Larsen & Riisgård (1994) therefore, considered the sponge pump as a viscous peristaltic model pump with nonlinear characteristics. In equation (7), they used $Q_L = c_1 \Delta H_p$ (on the assumption of linear leakage) and $Q_p = c_2 - c_3(\Delta H_p)^2$ (on the assumption that frequency and amplitude of the flagellae decrease nonlinearly with increasing pressure). Here, c_1, c_2 and c_3 are constants that were determined, using equations (7) and (14), to match the measured back-pressure

characteristic. Figure 4 shows the resulting model characteristics for pump (dashed curve) and back-pressure (solid curve). Further theoretical study and experimental results are needed to clarify the postulated phenomenological pump model for the bundles of flagella in choanocyte chambers, which appear to deliver a surprisingly high pressure rise.

III. POLYCHAETES

Adaptations to filter-feeding have independently evolved in different groups of polychaetes as illustrated with the following three examples of quite different polychaetes.

(1) Sabella penicillus

The polychaete *Sabella penicillus* lives in a tube, which it builds from suspended mud (Fig. 5*a*). The feeding mechanism in *S. penicillus* has been described by Nicol (1931). The feeding organ is composed of two lateral lobes which are joined at the base on the dorsal side only. They curve around both sides of the mouth (Orrhage, 1980), and each bears numerous filaments which stand out stiffly at regular intervals to form a crown. Each filament bears a double row of alternating pinnules (Fig. 5*b*). Water is drawn into the interpinnule canals from the outside by the beating of compound latero-frontal cilia each consisting of 5 or 6 single cilia (Fig. 5*c*, *d*). Along with this water stream enters suspended food particles, mainly algal cells. By means of still unknown mechanisms, food particles in the water are retained (downstream particle retention) and carried toward the mouth in a surface current produced by the frontal cilia (Mayer, 1994).

In order to analyse the ciliary crown-filament-pump of *Sabella penicillus* Riisgård & Ivarsson (1990) used the dimensions shown in Fig. 5 to define a 'standard' 65 mg dry weight worm, having 39 crown-filaments. From these data and the measured filtration rate, the mean water velocity (u) between the pinnules at 5, 10, 15 and 20 °C was estimated (Table 1).

The system characteristic in *Sabella penicillus* was calculated as the sum of only two contributions of importance, namely the pressure drop across the pinnule-lattice of the crown-filaments, ΔH_{ipc}, and the kinetic loss, ΔH_k, of the water leaving each crown-filament, which may be regarded as one of 39 parallel arranged 'pump units'. The structure of the crown-filaments approximates that of a filter consisting of parallel circular cylinders, the pinnules ($d = 35\ \mu m$), spaced with a distance, $b = 110\ \mu m$, between centre of neighbouring cylinders. Both equation (16) and (18) were used by Riisgård & Ivarsson (1990) to predict the pressure drop across the crown-filament. The calculated pressure drops are shown in Table 1. There is fairly good agreement between the two sets of estimates, and a mean value was used for calculating the operating point. The kinetic component was calculated to be $6{\cdot}5 \times 10^{-5}$ mm H_2O at 15 °C, using a mean velocity (u_{ex}) in the exhalant split of the crown-filament estimated as: (filament volume flow rate)/(filament 'exhalant area') = 1·11 mm s^{-1}.

The calculated components and operating points for 5, 10, 15 and 20 °C are shown in Table 1. There was a decrease in the operating point from 0·0246 to 0·0217 mm H_2O when the temperature was increased from 5 to 20 °C. The power output, P_p, from the *Sabella penicillus* pump was calculated by means of equation (24) at the four reference temperatures, as also shown in Table 1. The pump power (0·451 μW at 15 °C) was compared to the total metabolic energy expenditure of the 'standard' *S. penicillus*, as

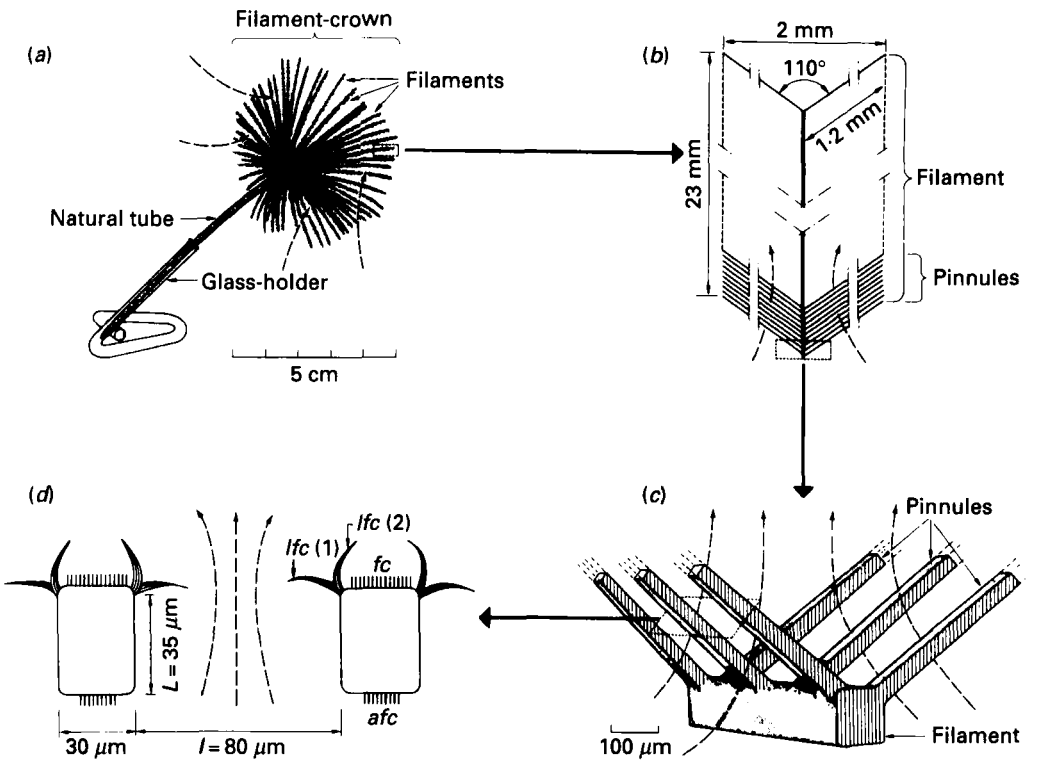

Fig. 5. *Sabella penicillus*. (*a*) Glass-holder with a worm within its natural tube and with the water pumping and particle capturing filament-crown extended. (*b*) Filament with two rows of pinnules branching off from the filament. (*c*) Idealized 'model' of section of filament with pinnules. (*d*) Cross section of two pinnules with latero-frontal cilia in resting position at end of recovery stroke, lfc(1), and end of active stroke, lfc(2); frontal cilia, fc; abfrontal-cilia, afc. Dimensions refer to a 'standard' 65 mg dry weight worm. Dashed lines indicate water flow due to the pumping activity of the latero-frontal cilia. (From Riisgård & Ivarsson, 1990).

Table 1. Sabella penicillus. *Volume flow rate (measured as volume of water cleared of 6 μm algal cells per unit time) in an optimally pumping 'standard' worm at reference temperatures of 5, 10, 15 and 20 °C. Interpinnule water velocity (u), the head losses, operating pressure (ΔH_{op}), power output (P_{op}) and efficiency (P_{op}/R_{tot}) are shown. (From Riisgård & Ivarsson, 1990).*

	5 °C	10 °C	15 °C	20 °C
Volume flow rate Q_{op} (ml s^{-1})	1·67	1·88	2·00	2·17
Water velocity u (mm s^{-1})	1·063	1·169	1·276	1·382
Head losses (mm H_2O)				
Interpinnule canals ΔH_{ips}				
equation (16)	0·021663	0·020587	0·019713	0·019040
equation (18)	0·027319	0·025963	0·024860	0·024012
Mean	0·024491	0·023275	0·0222865	0·021526
Kinetic loss ΔH_k	0·000045	0·000055	0·000065	0·000077
Operating pressure ΔH_{op}	0·0246	0·0234	0·0224	0·0217
Pumping power P_{op} (μW)	0·414	0·443	0·451	0·473
Efficiency P_{op}/R_{tot} (%)	0·370	0·396	0·402	0·423

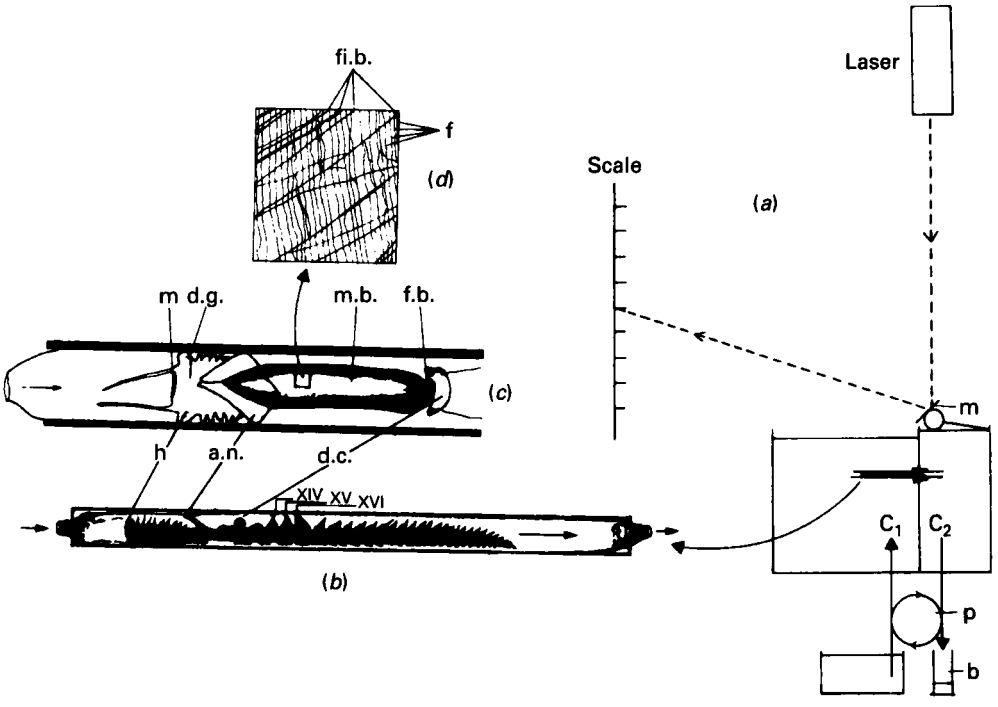

Fig. 6. (*a*) Experimental set-up used for direct measurement of pumping rates at different hydrostatic pressures imposed between inlet and outlet end of glass tube with *Chaetopterus variopedatus* inserted in the wall separating the inhalant (C_1) and exhalant chamber (C_2). The water level in C_2 is monitored with a laser beam striking a mirror (*m*) that is fixed on a tethered floating ping-pong ball. The pumping rate of the animal is equal to the volume of water collected in the beaker (*b*) per unit of time by means of the pump (*p*) when the laser deflection point is maintained fixed on the scale. (*b*) Lateral view of *C. variopedatus* in a glass tube lined with natural tube material. The water-pumping parapods (XIV, XV, XVI) produce a water current through the tube via the inlet and outlet terminal constrictions. (*c*) Dorsal view of anterior end of *C. variopedatus* lodged in a glass tube. Behind the head (*h*) the mucous net-bag (m.b.) is stretched out between the aliform notopodia (a.n.), which secrete the mucous bag, and the dorsal cupula (d.c.) within which the mucous net is being rolled up as a food ball (f.b.). At regular intervals the animal stops pumping and contracts, and the food ball is then transported via the dorsal ciliated groove (d.g.) to the mouth (*m*). (*d*) Structure of mucous net of *C. variopedatus* showing a rectangular mesh-work composed of an array of mostly parallel fibre bundles (fi.b.) perpendicular to an array of parallel filaments (f). (From Riisgård, 1989).

expressed by the oxygen consumption $R_{tot} = 0{\cdot}021$ ml $O_2 h^{-1}$ which corresponds to 112 μW. Using equation (25), the pump efficiency was found to be $\eta = 0{\cdot}4\,\%$. The efficiencies listed in Table 1 for other temperatures are based on the same value of total metabolic energy expenditure.

(2) Chaetopterus variopedatus

This polychaete lives in a parchment-like tube, which it secretes. The mucous-net filter-feeding of the worm has been described, and different aspects of water pumping and particle retention have been studied (MacGinitie, 1939; Wells & Dales, 1951; Brown 1975, 1977; Flood & Fiala-Médioni, 1982; Jørgensen *et al.*, 1984; Riisgård, 1989). The feeding method may be summarized as follows.

A flow of water through the tube is driven in the antero-posterior direction by three muscular piston-like parapods in the middle region of the body (segments no. 14, 15 and 16, see Fig. 6*b*). Two aliform notopodia (segment no. 12) continuously secrete a mucous net-bag which filters the water current. The posterior end of the suspended mucous net-bag is rolled up into a food ball within the dorsal capsule, a ciliated cup-like organ (segment no. 13), and is ingested at intervals of 15–20 min (MacGinitie, 1939). The mucous net is built of longitudinal parallel fibre bundles and transverse filaments forming a rectangular mesh (Flood & Fiala-Médioni, 1982) which efficiently retains suspended food particles down to *c.* 1 μm (Jørgensen *et al.*, 1984).

Typical measured back-pressure characteristics for *Chaetopterus variopedatus* (Fig. 7*a*, Riisgård, 1989) suggest a piston-type pump behaviour with increasing leakage and decreasing stroke frequency as the back pressure, hence the necessary pump pressure, increases. Based on several such observations, Riisgård (1989) considered a 'standard' *C. variopedatus* (50 mg dry weight) within a 10 cm long glass tube (inner diameter = 6·7 mm, with two terminal circular constrictions of radius $r = 1{\cdot}1$ mm). The pumping rate at zero back pressure was $Q_{op} = 300$ μl s^{-1} at $f = 60$ strokes min^{-1}, and the maximal pressure rise at zero flow was $\Delta H^0_{12} = 6$ mm H_2O.

To determine the pump power, using equation (6), the pressure head at the normal operating point (ΔH_{op}) was calculated from estimates of the system resistances, comprising primarily the mucous net-bag, channel flows and kinetic losses. The pressure drop across the mucous net was found as follows. The area of the mucous net-bag of the 'standard' worm was estimated to be 2 cm^2, and with a pumping rate of 300 μl s^{-1} the corresponding mean velocity was $u_\infty = 0{\cdot}3/2 = 0{\cdot}15$ cm s^{-1}. The fine structure of the mucous net was studied by Flood & Fiala-Médioni (1982), using transmission electron microscopy, and the net appeared to be a rectangular mesh consisting of one array of mostly parallel fibre bundles, composed of 3 to 10 fibres, with a spacing of $0{\cdot}76 \pm 0{\cdot}96$ μm in one direction and perpendicular to this system a second array of parallel filaments spaced by relatively constant intervals of $0{\cdot}46 \pm 0{\cdot}12$ μm. Each fibre bundle was about 0·1 μm thick and the filaments range in diameter between 10 to 30 nm. A pore width of less than 0·5 μm was thus suggested. However, the particle retention spectrum measured by Jørgensen *et al.* (1984) suggested a 3 × larger mesh size (i.e. $2{\cdot}3 \times 1{\cdot}4$ μm) because only particles down to about 1·5 μm are retained with 100% efficiency. The exact mesh size of the *in vivo* mucous net is therefore unknown. The pressure drop across a net with a mesh size of $2{\cdot}3 \times 1{\cdot}4$ μm and a supposed mean filament diameter of 20 nm was calculated by Riisgård (1989) by means of equation (17), yielding $\Delta H_m = 0{\cdot}72$ mm H_2O and is considered to be representative of the *in vivo* situation.

The kinetic losses of restrictions was taken to amount to two contributions of equation (22) referred to the volume flow leaving the restrictions of the glass tube. Hence, $u_{ex} = 0{\cdot}3/(\pi \times 0{\cdot}11^2) = 7{\cdot}89$ cm s^{-1}, and the total kinetic loss in the two constrictions was thus $\Delta H_{ex} = u^2_{ex}/g = 0{\cdot}64$ mm H_2O. The frictional head loss was simply estimated as that of fully developed flow through the empty glass tube. Using equation (19) this gave $\Delta H_f = 0{\cdot}07$ mm H_2O. Adding the three contributions gives the total head loss along the flow path from inlet to outlet at the normal operating point, $\Delta H_{op} = 0{\cdot}72 + 0{\cdot}64 + 0{\cdot}07 = 1{\cdot}43$ mm H_2O. Making an assumption about the function $g(Q/Q_{op})$ in equation (11), and scaling the above head losses at the normal operating

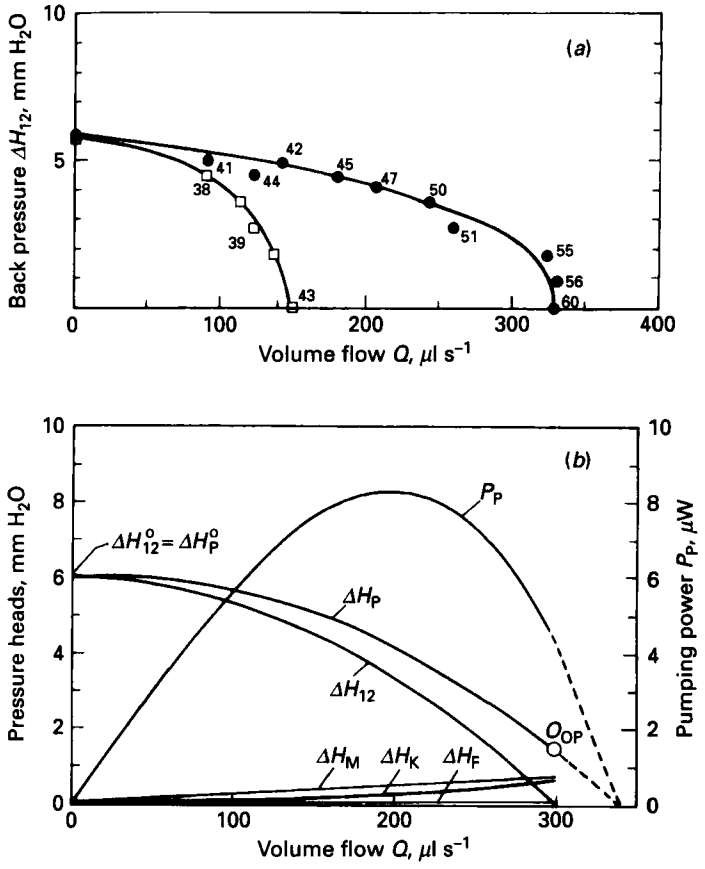

Fig. 7. *Chaetopterus variopedatus*. (*a*) Back pressure-pumping rate characteristic measured in two experiments performed on different days on which the stroke frequency of the water pumping parapods at zero back pressure was 43 (□) and 60 (●) strokes min^{-1}, respectively. The stroke frequency of the parapods, recorded simultaneously with the direct measurement of the pumping rate at different back pressure, is indicated. (*b*) Pressure head-pumping rate characteristics for pump pressure (ΔH_p) and the different components in the system resistance: mucous bag (ΔH_m), kinetic loss (ΔH_k), friction (ΔH_f) and back pressure (ΔH_{12}). P_p: pumping power-pumping rate characteristic of the pump. O_{op}: normal operating point. The calculations are based on a 'standard' *C. variopedatus* exploiting its water pumping capacity Q_{op} = 300 μl s^{-1}. (From Riisgård, 1989).

point to other flow rates according to equation (12) for the mucous net and friction, and according to equation (13) for restrictions, and using measured stroke frequency in equation (10), Riisgård (1989) also modelled the back-pressure characteristics from equation (14), which are shown in Figure 7*a* (solid lines). Finally, the useful work done by the pump, P_{op} = 4·3 μW according to equation (24), was compared to the total metabolic energy expenditure of a 'standard' *C. variopedatus*, as expressed by the rate of oxygen consumption R_{tot} = 0·02 ml O_2 h^{-1} which corresponds to 107 μW. Thus, the useful work done by the pump constituted η = 4 % of the total metabolic rate.

(3) Nereis diversicolor

The common and abundant polychaete *Nereis diversicolor* lives on shallow soft-bottoms in north-western Europe. The worm is almost entirely restricted to the littoral zone where it lives in a U-shaped burrow in the sediment. *N. diversicolor* has been described as a carnivore and/or scavenger, but also as a suspension-feeder and a detritivore, feeding partly by swallowing surface mud around the openings of the burrow (Wells & Dales, 1951; Goerke, 1966; Evans, 1971). The occurrence of a filter-feeding mechanism in *N. diversicolor* was first described by Harley (1950), and later confirmed by Goerke (1966). Observations of filter-feeding behaviour were made by Riisgård (1991 *a*) on *N. diversicolor* in glass tubes immersed in seawater (Fig. 8). When a suspension of algal cells was added, the worm moved, within 5–15 min, to one end of the glass tube. There it fixed mucous threads to the glass wall, forming the circular opening of a net bag, which was completed as the worm slowly retreated down the tube, moving the anterior end from side to side in semi-circles. While making the funnel-shaped net-bag, and for a period after the bag was completed, the worm pumped water through the net by means of vigorously undulating movements of the body. Particles suspended in the inhalant water were retained by the net and after a certain period of pumping the worm moved forward, swallowing the net bag and its entrapped food particles.

In *Nereis diversicolor* the pumping action is a result of the undulating motion of the body within the tube. Observations indicate three posteriorly propagating waves in different phases, one of which creates an effective stroke for the pump. The effective wave peaks make firm contact with the tube wall both with the dorsal and ventral surfaces, suggesting good seals. On the lateral sides, the parapodia make contact to the sidewalls of the tube, forming less perfect seals which may leak with increasing back pressure. Riisgård *et al.* (1992) found that a pump design such as this resembled a positive displacement pump that leaks more and more as back-pressure is increased, and the suggestion also agreed with the general form of experimental back-pressure characteristics measured by Riisgård (1991 *a*). The *Nereis*-pump was therefore modelled by Riisgård *et al.* (1992) as the positive displacement leaking unit shown in Fig. 9 using equation (7) explicitly. Here, the flow due to pumping action, given by equation (10), was assumed to depend only on the experimentally determined stroke frequency, while the leakage flow was modelled by the expression

$$Q_L = C_L A_L \Delta H_P / \nu, \tag{33}$$

where A_L denotes the slit area through which viscous leakage flow is driven by excess pressure (ΔH_P) and C_L is a constant. The kinematic viscosity, ν, was included to study the effect of temperature on the pump, recall equation (26). The available area, A_L, for leakage flow is not constant but increases with increasing excess pressure. Furthermore, the valve opening may be retarded at increasing stroke frequency. Therefore, the resulting reduction in amplitude of valve opening was modelled as a mechanical system for which the amplitude depends on the ratio f/f_r, where f_r denotes a reference frequency. Due to lack of further information, Riisgård *et al.* (1992) assumed a simple model in which it was supposed that the valve area was dependent linearly on excess pressure and inversely dependent on frequency as $A_L \approx \Delta H_P/[1+(f/f_r)^2]$.

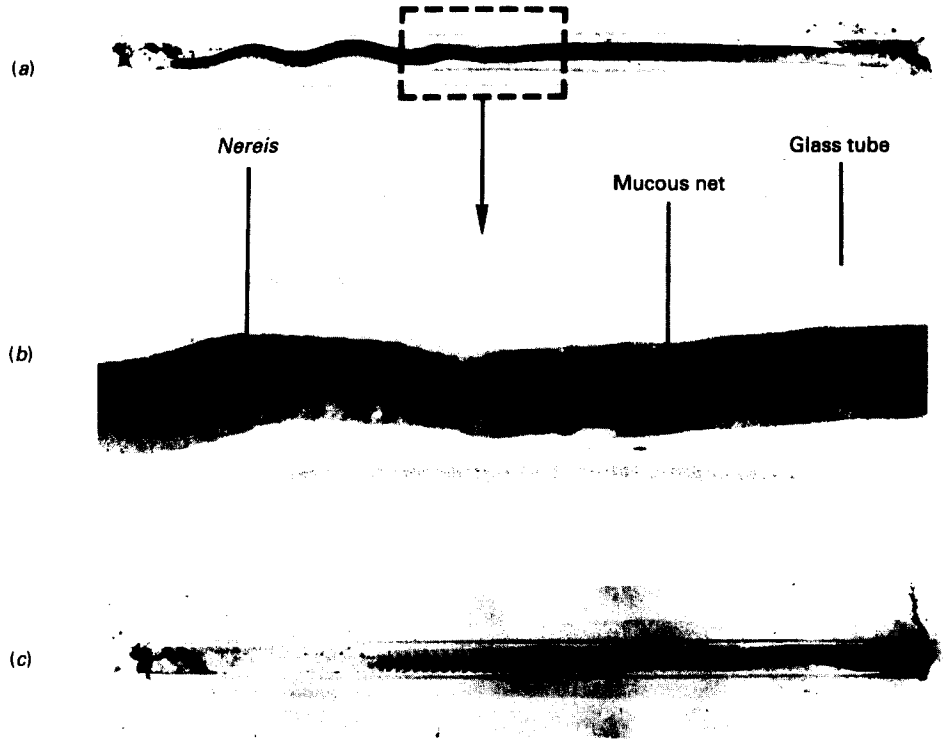

Fig. 8. *Nereis diversicolor*. (*a*) Photograph of *N. diversicolor* lodged in a glass tube (length = 12 cm). The worm is seen from the side so that the undulating body movements, which produce a water current through the tube, can be seen. When the water passes through the tube it is filtered through a mucous net bag which has been made visible by means of suspended carmine powder. (*b*) Magnification of anterior end of the same worm as shown in (*a*). (*c*) Near dorsal-ventral view of the worm while swallowing the mucous net bag 3 min after photograph (*a*) was taken. (From Riisgård, 1991*a*).

The leakage flow modelled above is interesting because it implies that the nonlinear function $g(Q/Q_p^0)$ in equation (11) involves the factor $[f/f_r - Q/Q_p^0]^{\frac{1}{2}}$ which, through equation (14), reappears in the model for the back-pressure characteristic, giving the experimentally observed curvature. To complete the model, the system head losses were calculated from standard equations on the basis of the known geometry of the flow system.

To examine experimental data in light of the proposed pump model Riisgård *et al.* (1992) defined two 'standard' individuals to be representative of *Nereis diversicolor*. One was denoted 'low gear' (with frequency decreasing from a maximum of 70 to about 50 strokes min^{-1} at increasing back pressure). The other was a 'high gear' individual (with frequency decreasing from a maximum of 90 to about 70 strokes min^{-1}). Geometry, net bag, and tube were the same for both individuals, while volume flow Q_{op} at standard condition (15 °C) was 115 and 140 $\mu l\ s^{-1}$, respectively (Table 2). Using equation (17), the pressure drop over the mucous net was found to be ΔH_n = 0·336 and 0·409 mm H_2O, respectively, for 'low' and 'high gear' individuals. Additional contributions to the frictional pressure drop were derived from flow in the part of the

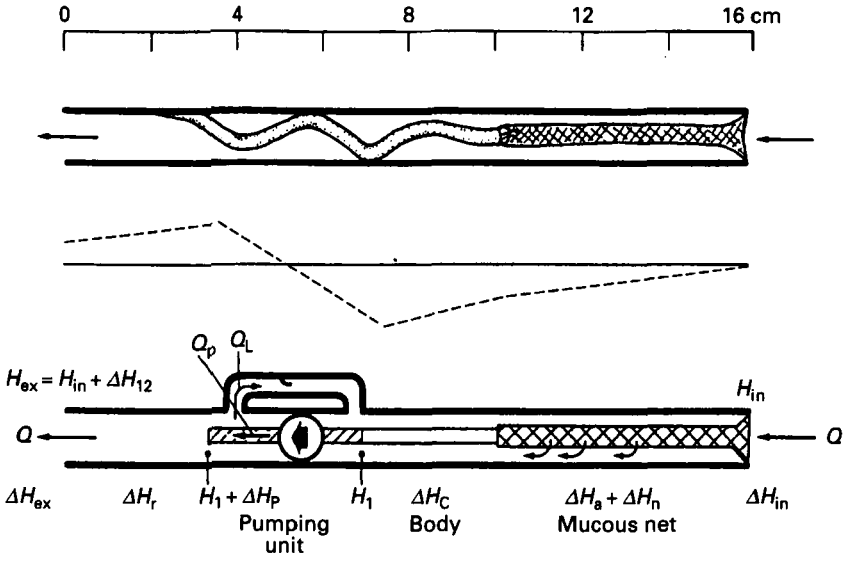

Fig. 9. *Nereis diversicolor*. Schematic illustration of suspension feeding worm in its tube (top), pressure above inlet value versus flow path (middle), and model (bottom), showing frictional pressure drop at the inlet ΔH_{in}, across the mucous net ΔH_n, in the annular space between net and tube ΔH_a, in flow past body ΔH_C, in a length of tube ΔH_r, and at the exit ΔH_{ex}. The positive displacement pumping unit, delivering flow Q_P at pressure rise ΔH_P, has an internal leakage flow Q_L passed the sealing parapodia, yielding net volume flow $Q = Q_P - Q_L$ against internal losses and externally imposed back pressure ΔH_{12}. (From Riisgård *et al.*, 1992).

Table 2. Nereis diversicolor. *Pump model parameters of 'standard' worms at* 15 °C (*From Riisgård* et al., 1992)

Parameter	'Low gear'	'High gear'
From experiments (Riisgård, 1991 *a*)		
Q_{op} (μl s^{-1})	115	140
f_0 (strokes min^{-1})	70	90
$f(0)$ (strokes min^{-1})	50	70
ΔH_{12}^0 (mm H_2O)	8	10
Predicted frictional pressure drop (mm H_2O) at normal conditions		
ΔH_a	0·278	0·330
ΔH_n	0·336	0·409
ΔH_r	0·088	0·108
ΔH_e	0·526	0·640
ΔH_{f0} (total)	1·228	1·487

tube not occupied by the worm (ΔH_r), through the annular space between worm and tube (ΔH_e), and those spaces parallel to the net, both inside and outside the bag (ΔH_a), see Fig. 9. The calculated values of these contributions and their sum, the total frictional pressure drop (ΔH_{f0}), as well as other parameters of 'low gear' and 'high gear' worms, are listed in Table 2.

The operating pressure, ΔH_{op}, of the *Nereis diversicolor* pump was found by adding the kinetic loss ΔH_{ex} to ΔH_{f0} (see Table 2). The exit loss for the 'standard high gear'

N. diversicolor was found from using equation (22) as 0·0057 mm H_2O, and thus ΔH_{op} = 1·487+0·0057 = 1·493 mm H_2O. The power output from the pump was then calculated from equation (24) to be P_{op} = 2·10 μW. With a metabolic rate R_{tot} = 12·6 μl O_2 h^{-1} (Riisgård, 1991*a*) equivalent to 70 μW, the useful pump work was found to be η = 3 % of the total metabolic energy expenditure of the individual (Riisgård *et al.*, 1992).

IV. BIVALVES

(1) *Water pumping and particle retention*

The bivalves constitute the most studied group of filter-feeding animals, but the basic mechanisms of water pumping and particle retention is still incompletely understood (Jørgensen, 1990; Nielsen *et al.*, 1993). In the blue mussel, *Mytilus edulis*, bands of lateral cilia produce the main water transport through the interfilamentary canals of the gill (Fig. 10). Near the entrance to the canals, particles are separated from the main currents and transferred into frontal surface currents driven by the frontal cilia. The latero-frontal cirri, located at the entrance to the interfilamentary canals, have a fixed pattern of alternating beat which suggests that they play an active part in the separation process. The absence, however, of the latero-frontal cirri in other bivalve gills, i.e. the Microciliobranchia excluding the Ostreidae (Owen & McCrae, 1976), and all other upstream-collecting systems (Nielsen, 1987), indicates that the latero-frontal cirri may be a speciality of some bivalves to improve their retention efficiency for smaller particles (Vahl, 1973; Møhlenberg & Riisgård, 1978; Riisgård, 1988*b*). Particle trajectories near an isolated *M. edulis* gill filament were video-recorded by Nielsen *et al.* (1993). The particle tracks indicated that the latero-frontal cirri play a role in the transfer of particles from the through current to the frontal current, probably by means of a strong interaction through the motion of intervening fluid rather than through a direct physical contact.

(2) *Pump characteristics, energetics and modelling*

In filter-feeding bivalves, represented by the mussel *Mytilus edulis*, the system resistance was resolved by Jørgensen *et al.* (1986*a*) into the following components:

$$\Delta H_s = \Delta H_f + \Delta H_{ex} + \Delta H_{lf} + \Delta H_{12}, \tag{34}$$

which is equation (4) with the added term ΔH_{lf}, representing the resistance due to the beating of the latero-frontal cirri against the through-flow. The back pressure characteristic was experimentally determined as a linear function (Fig. 11), and thus could be described by the relation

$$\Delta H_{12} = \Delta H_{12}^0(1 - Q/Q_{op}), \tag{35}$$

where $\Delta H_{12}^0 = \Delta H_p^0$ is the maximum pressure head (at zero flow).

To evaluate the contribution of the latero-frontal cirri to the system resistance, Jørgensen *et al.* (1986*a*) studied the effect of the nerve transmitter serotonin. When serotonin is added to the ambient water in a concentration of 10^{-5} M it affects the functioning of the cirri by fixing them at the end of the effective stroke thus removing them from the flow path and eliminating their contribution to the frictional loss. From Fig. 11, it appears the serotonin treatment had no measurable effect on the back pressure characteristic and the term ΔH_{lf} was therefore omitted. Assuming that the

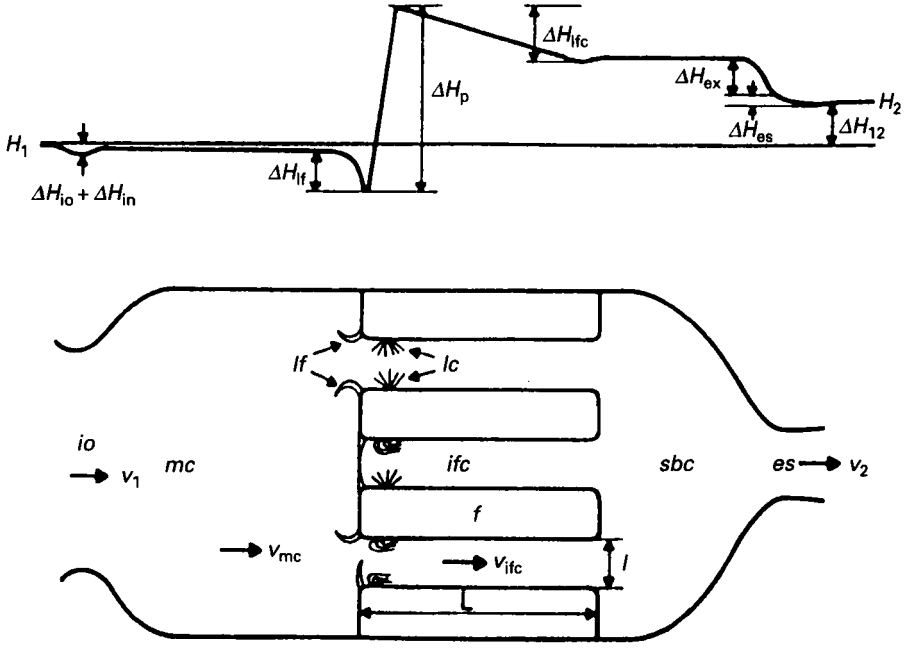

Fig. 10. *Mytilus edulis*. Diagrams of the mussel pump and pressure heads (ΔH, top figure) along the flow path. io = inhalant opening, mc = mantle cavity, sbc = suprabranchial cavity, es = exhalant siphon, f = gill filament, L = length of filament, l = interfilament distance, lf = latero-frontal cirri, lc = lateral cilia v_1 = flow velocity in inhalant opening, v_2 = flow velocity in exhalant siphon, v_{ifc} = flow velocity in interfilament canals, v_{mc} = flow velocity in mantle cavity. (From Jørgensen *et al.*, 1986*a*).

serotonin treatment did not affect the lateral cilia, believed to constitute the pump, this could mean that the latero-frontal cirri during normal operation contribute to the pumping by the same amount as they contribute to the resistance to flow.

The other elements of the system characteristic were determined by Jørgensen *et al.* (1986*a*) as briefly described in the following (see Fig. 10). The mean velocity in the inter-filament canals, filling up 50% of the gill area, was found to be u_{ifc} = (filtration rate)/(0·5 × gill area) = 1000/(0·5 × 850) = 2·36 mm s^{-1}. The frictional loss in the inter-filament canals (regarded as stationary parallel plates with length L = 200 μm and spaced a distance l = 40 μm apart) was then calculated from equation (21) to be ΔH_{ifc} = 0·44 mm H_2O. The mean velocity of the jet through the oval siphonal aperture with a cross-sectional area of 16 mm^2 was u_{ex} = 1000/16 = 62·5 mm s^{-1} and the kinetic energy head loss was then calculated by using equation (22) to be ΔH_{ex} = 0·38 mm H_2O. The head loss over the inhalant opening was estimated to be ΔH_{io} = 0·02 mm H_2O. The frictional pressure drop in the inhalant opening (ΔH_{in}) and the short exhalant siphon (ΔH_{es}) was estimated from boundary layer theory (see text following equation (21)) to be 0·004 and 0·14 mm H_2O respectively. The normal operating pressure of the pump, estimated as the total head loss along the flow path from entry to exit in a 35 mm 'standard' mussel, was thus found to be: ΔH_{op} = 0·004 + 0·02 + 0·44 + 0·14 + 0·38 ≈ 1 mm H_2O. Knowing the pumping rate of the 'standard' mussel in the fully open state (Q_{op} = 1 ml s^{-1}), the useful pumping power was estimated from equation (24) to be P_{op} = 10 μW. With a metabolic rate of R_{tot} = 900 μW, the overall pump efficiency was η = 1·1% (Jørgensen *et al.*, 1986*a*, 1988). Further studies of the properties of the

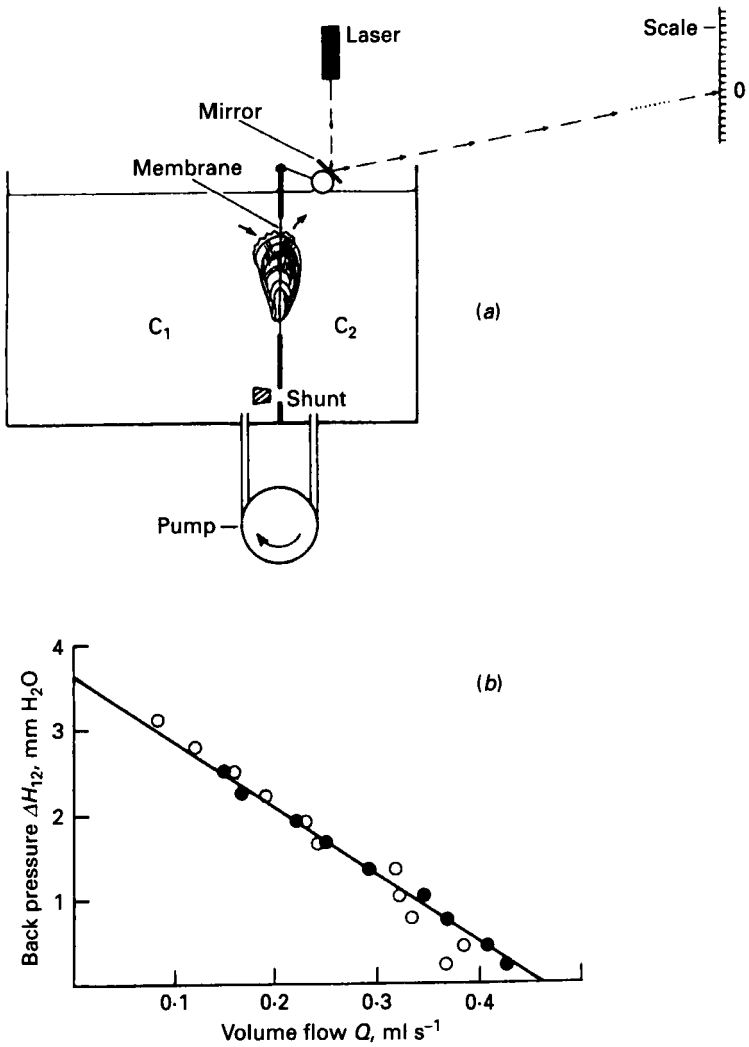

Fig. 11. (*a*) Set-up for direct measurements of pumping rates in the mussel *Mytilus edulis*. When the shunt is closed the mussel builds up a certain known back-pressure (read on scale), and when the reflected laser-spot on the scale is kept fixed by means of the calibrated pump, the pumping rate of the mussel and the mechanical pump is identical. (*b*) Back-pressure pumping-rate characteristic in a mussel pumping seawater (closed symbols) and seawater containing serotonin (open symbols) which removes the laterofrontal cilia from the through-current. It is seen that the removal of the cirri did not cause increased pumping rate thus indicating an insignificant contribution of the cirri to the system resistance. (From Jørgensen *et al.*, 1986).

mussel pump and more extensive modelling have been carried out by Jørgensen *et al.* (1988, 1990), and the literature on bivalve filter-feeding hydrodynamics and energetics has recently been reviewed by Jørgensen (1989, 1990).

The gill pump is basically similar in all filter-feeding bivalves. It consists of opposing bands of lateral cilia running along the filament sides close to the entrance to the interfilament canals. As stated above, the most important contributions to the operating pressure in *Mytilus edulis* derive from the frictional pressure drop in the interfilament

canals and the exit loss. Because *M. edulis* lacks an inhalant siphon and the exhalant siphon is short, it has been of interest to assess the resistance in the long siphons of the infaunal soft clam *Mya arenaria*. Jørgensen & Riisgård (1988) attempted to estimate the resistance in the siphons of *M. arenaria* to water flow using two independent approaches. One approach was to study the effect on pumping rate when the siphons of *M. arenaria* were excised at the base. If the siphons constitute a substantial resistance, the pumping rate should increase as a consequence of the operation. It was found that excision of the siphons had no measurable effect on the pumping rate. The other approach was theoretical. The siphons are tubes of approximately constant, circular cross-sectional areas along their entire length, and the frictional resistance could be calculated from equation (19). The calculations were based on a clam pumping 1 ml s^{-1} with the siphons extended to a length of 10 cm. With internal diameters of 0·7 and 0·6 cm of the inhalant and exhalant siphons, respectively, the total siphon resistance amounted to $\Delta H_{fs} = 0{\cdot}21 + 0{\cdot}38 = 0{\cdot}59$ mm H_2O. Thus, the calculations indicated that the resistance to water flow in the *M. arenaria* siphons is relatively high, not in close agreement with the experimental findings (possibly due to reduced filtration rate of the operated clams). With an exhalant siphon aperture diameter of 4 mm the velocity of water leaving the clam was estimated as $u_{ex} = 1/\pi 0{\cdot}2^2 = 8{\cdot}0$ cm s^{-1} and equation (22) gave the kinetic head loss $\Delta H_{ex} = 0{\cdot}3$ mm H_2O. Assuming a frictional resistance in the interfilament canals of the gills to be $\Delta H_{ifc} = 0{\cdot}44$ mm H_2O (as in *Mytilus edulis*) the operating pressure amounted to $\Delta H_{op} = \Delta H_{fs} + \Delta H_{ifc} + \Delta H_{ex} = 0{\cdot}59 + 0{\cdot}44 + 0{\cdot}3 = 1{\cdot}33$ mm H_2O. This value indicates that *M. arenaria* and *M. edulis* (and other ciliary gill pumps in filter feeding bivalves) may have a near identical normal operating pump pressure of approximately 1 mm H_2O.

(3) *Interpretation problems*

A vast number of measurements about bivalve filtration rates have been carried out since the beginning of the century, but basic questions still cause controversy in the literature (e.g. Riisgård, 1991*b*). This is an indication of the difficulties of creating optimal conditions in the laboratory, including establishing a proper food regime to which the bivalves are adapted. Thus, growth rates comparable with those observed in nature may only be obtained in laboratory experiments when these are carried out at algal concentration to which the bivalves are adapted. Unnaturally high algal concentrations may lead to suboptimal conditions (partial valve closure, reduced metabolism and reduced growth). This condition seems to have been largely ignored. The wide range of results stresses the importance of performing laboratory experiments under optimal conditions, including natural algal concentrations at which the pumping capacity is exploited. This is necessary in order to interpret laboratory findings in a meaningful physiological context (Jørgensen, 1990; Riisgård, 1991*b*; Nielsen *et al.*, 1993).

Some recent studies of the *Mytilus edulis* pump have been directed to examination of the relationship between valve gape and pump characteristics. The effects of progressively reduced valve gape on the back pressure-pumping rate characteristic was studied by Jørgensen *et al.* (1988) who found that pumping pressure and pumping rate are both reduced proportionately at reduced valve gape. This was interpreted to be due to a shortening of the gill axes leading to a reduction in width of the interfilament canals

(see Fig. 10 in Jørgensen, 1989), presumably because interference between opposing bands of water pumping lateral cilia becomes negative with decreasing width of the interfilament canals. The relationship between valve gape and filtration rate did not appear to be a mechanism of controlling filtration rate and thus food ingestion, but the reduction in filtration rate was interpreted as a secondary effect of the mussels response to suboptimal conditions.

The purpose of water pumping in filter-feeding bivalves is primarily to secure food, but it also ensures the necessary oxygen uptake. The gills are feeding structures which pump water at rates appropriate to the level of phytoplankton in the surrounding water and the bivalve pump is thus the evolutionary result of the interaction between the organism and its biotope. The evolutionary transition of the gills from respiratory organs to feeding structures involved an increase in ventilatory capacity of the organism. Experiments have shown that oxygen consumption is closely correlated to pumping rates in the lower flow rates, representing pumping rates under suboptimal conditions, but not to the higher pumping rates (Jørgensen *et al.*, 1986*b*). The relationship between oxygen consumption and pumping rate has previously been interpreted with respect to the metabolic cost of water transport (Verduin, 1969; Bayne, Thompson & Widdows, 1976; Bernard & Noakes, 1990). Such interpretations have been criticized by Jørgensen (1992) as 'lacking biological meaning', because the relationship can be explained in physical terms due to the flow rate dependent resistance to oxygen diffusion across the boundary layers along the surfaces of oxygen uptake. At low pumping rates the boundary layers are thick, but at increasing pumping rates, the thickness decreases, and the resistance to oxygen uptake is no longer controlled by the boundary layers.

V. ASCIDIANS

Benthic, filter-feeding ascidians pump water through the pharynx which is perforated with small slits; the stigmata. Ciliary tracts on either side of the stigmata create a water current which runs through the inhalant siphon into the pharyngeal chamber and through the stigmata into the atrium from which the water leaves the ascidian as a jet through the exhalant siphon (Fig. 12). When the water is pumped across the pharynx wall, suspended particles are trapped on the mucous net continuously produced by the endostyle (Holley, 1986). Cilia on the papillae or longitudinal pharyngeal bars transport the endless mucous net, with the retained food particles, to the dorsal lamina where it is rolled into a cord which is passed posteriorly into the esophagus as an unbroken string (MacGinitie, 1939; Millar, 1971; Fiala-Médioni, 1978). Thus, the amount of food available to ascidians is determined by the efficiency with which the particles are retained by the mucous net, by the amount of water pumped through the pharynx and by the concentration of food particles in the water. Particles down to 2–3 μm are completely retained (Randløv & Riisgård, 1979; Jørgensen *et al.*, 1984), and electron microscopic studies of the mucous net have revealed that in the fixed state, it is composed of 10–40 nm thick fibres arranged in rectangular meshes that vary between 0·2 and 0·5 μm in width and between 0·5 and 2·2 μm in length (Flood & Fiala-Médioni, 1981). The ascidian pump and the energy expenditure of pumping large amounts of water through a mucous net, which efficiently retains particles down to a few microns, has been studied by Riisgård (1988*a*).

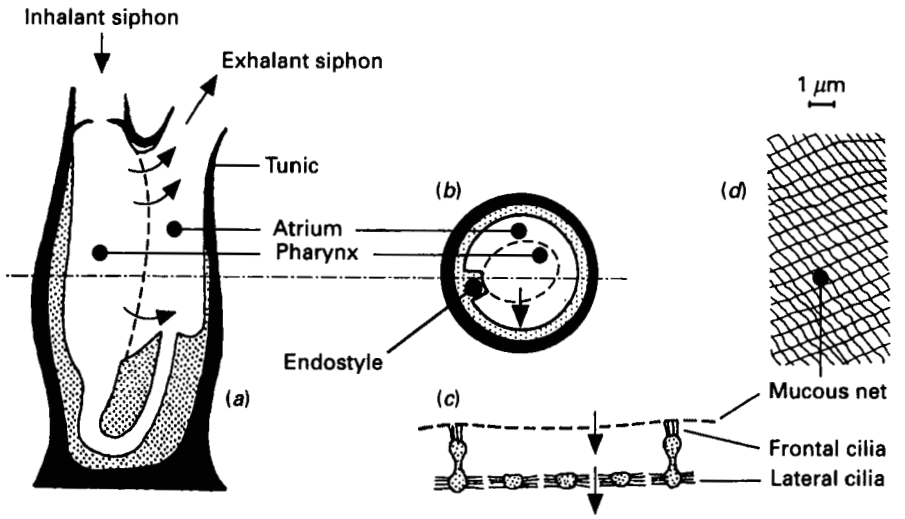

Fig. 12. Diagrammatic longitudinal (*a*) and transverse (*b*) sections, and a magnified section through the part of wall of the pharynx (*c*) of a typical ascidian (From McNeill Alexander, 1975) pumping water (arrows) through a rectangular mucous net (*d*); drawing based on EM picture of mucous net produced by *Ciona intestinalis* (From Flood & Fiala-Médioni, 1981).

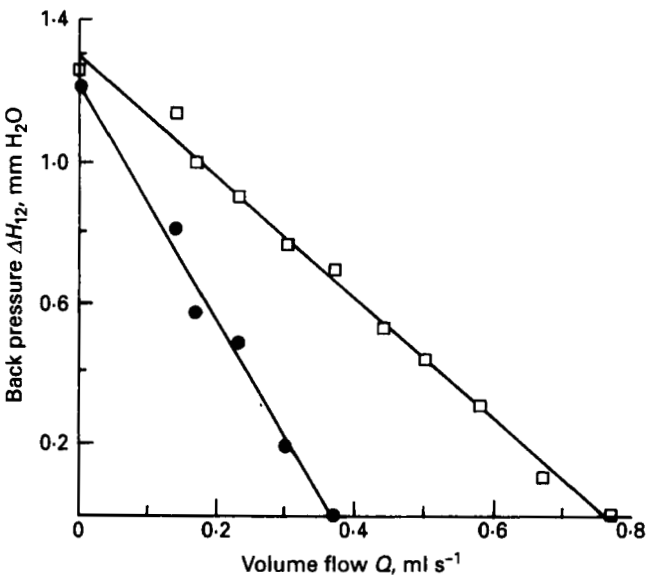

Fig. 13. *Styela clava*. Back-pressure pumping-rate characteristic in two ascidians with different size (open symbols: 0·412 g total dry weight; closed symbols: 0·179 g dry wt) and pumping rate but near identical maximal pressure rise at zero volume flow. (From Riisgård, 1988*a*).

Figure 13 shows experimental results for *Styela clava* in terms of two typical back-pressure characteristics, which conformed to the linear relation of equation (35). The system resistance, equation (4), was resolved into the following components:

$$\Delta H_s = \Delta H_m + \Delta H_k + \Delta H_f + \Delta H_{12}, \tag{36}$$

ΔH_m = head loss across the mucous net, ΔH_k = sum of the kinetic energy loss as water enters the inhalant and leaves the exhalant siphon, ΔH_f = frictional resistance in the canal system, ΔH_{12} = back pressure.

In a 'standard' *Styela clava*, the diameter of inhalant and exhalant siphon apertures were 0·8 and 0·5 cm, respectively. With a pumping rate of 0·76 ml s^{-1}, the velocity in the siphons could be estimated, and using equation (23) with $K = 1$, the entrance and exit kinetic energy loss amounted to 0·012 and 0·076 mm H_2O, respectively. The frictional resistance in the inhalant and exhalant siphons, which were 1·2 and 1·0 cm long respectively, was calculated by using equation (19) which yielded 0·010 and 0·056 mm H_2O, respectively. The area of the pharynx wall was found from the contour of the pumping ascidian. Knowing also the pumping rate, the flow velocity at the mucous filter was found to be $u_\infty = 0{\cdot}30$ mm s^{-1} and the pressure drop across the net could be estimated from equation (16) to be $\Delta H_m = 0{\cdot}069$ mm H_2O. The sum of these 3 contributions to the total head loss along the flow path from entry to exit is thus $0{\cdot}088 + 0{\cdot}066 + 0{\cdot}069 = 0{\cdot}223$ mm H_2O. The resistances to flow in other parts of the pump system (i.e. pharynx chamber, pharyngeal stigmata and atrium) were not calculated, but the pressure losses over the pharynx chamber and atrium were assumed to be insignificant. The operating pressure was therefore presumed to be $\Delta H_{op} = 0{\cdot}3$ mm H_2O in the optimally working ascidian pump.

Ignoring the small kinetic head loss and introducing equation (6) and (35) into equation (36), the result may be written as the linear pump characteristic

$$\Delta H_p = \Delta H_{12}^0 - (\Delta H_{12}^0 - \Delta H_{op})\, Q/Q_{op}, \tag{37}$$

which corresponds to equation (9) for $Q_p^0 = Q_{op}(1 - \Delta H_{op}/\Delta H_p^0)^{-1}$ since $\Delta H_p^0 = \Delta H_{12}^0$. As illustrated by the numerical example above, the equation of the pump characteristic can be established by measuring ΔH_{12}^0 and Q_{op} and by deriving expressions for the head loss as function of volume flow using standard equations. Also, since equation (37) is linear in Q the useful power output of the pump (calculated from equation (24)) becomes a simple parabola. At the normal operating point of the 'standard' *Styela clava*, $P_{op} = 2{\cdot}3$ μW. The total metabolic energy expenditure of the ascidian, as expressed by the rate of oxygen consumption, was 0·167 ml O_2 h^{-1} which corresponds to $R_{tot} = 891$ μW, and the overall pump efficiency becomes $\eta = 0{\cdot}26\,\%$.

VI. CHARACTERISTICS OF MACRO-INVERTEBRATE FILTER-FEEDING

(1) *Energy cost of filter-feeding*

Filter-feeding may be characterized as a 'life in a nutritionally dilute environment' (Conover, 1968), and the low concentrations of small suspended food particles in the sea is the key to understanding the character of filter-feeding in marine macro-invertebrates. According to Jørgensen (1975), it may be assumed that filter-feeding evolved according to a principle of minimal dimensioning of the filter- and pump systems which enable continuous feeding at low rates, rather than discontinuous feeding at correspondingly high rates. The present review confirms this view which implies that filter-feeders possess low-energy (i.e. low-pressure) pumps that are continuously pumping the surrounding water through filter-structures which efficiently retain small suspended food particles.

The biological significance of energy cost of filter-feeding in marine macro-invertebrates may be evaluated on the basis of the overall pump efficiency estimated as useful pump power output related to the total metabolic output, $\eta = P_{op}/R_{tot}$ given as equation (25). For representatives of various taxonomic groups examined in the present paper, such results are given in Table 3 showing that the useful pump work constitutes between 0·26 % (*Styela clava*) and 4 % (*Chaetopterus variopedatus*) of total metabolic expenditure.

The overall pump efficiency may be useful as a general characterization of filter-feeders, but it ignores the aspects of power conversion associated with the pumping process. As emphasized by Jørgensen (1990), the energetics of the bivalve pump, for example, may be studied at several levels: (1) useful power output from pump, (2) energy consumed by the beating of the water-pumping lateral cilia, (3) energy consumed by the cells carrying the bands of lateral cilia, (4) energy consumed by the gills (the water processing structure) and (5) energy consumed by the whole animal (the global pump). Such a hierarchy gives rise to a number of efficiencies of energy transfer between levels, each of which may be of importance for understanding the energetics of filter-feeding. On the level below the intact animal (i.e. the global pump), it is necessary to be specific, possibly by following the schematic subdivision shown in Fig. 14 which reflects the five levels described above. Here, P_p at level (1) is the useful (reversible) power received by the water as calculated from equation (24). P_{mek} is the actual rate of mechanical work done on the fluid by the structures responsible for the pumping. The ratio of these two quantities defines the mechanical efficiency of the pump, $\eta_{mek} = P_p/P_{mek}$. Given the kinematics of the pump, this efficiency can in principle be found by a fluid mechanical analysis (see references below). Level (2) above is assumed to be the biochemical equivalent of P_{mek}, represented by the hydrolysis of ATP that takes place in the beating lateral cilia. The metabolic efficiency of level (3), i.e. the pump proper (the cells carrying the lateral cilia) is defined by $\eta_m = P_{mek}/R_p$ where R_p denotes the pump metabolic rate. Further, the cells carrying the cilia in the bivalve pump are part of larger structures, the gills, that are needed to form flow channels, etc. but may have other functions as well. The metabolic power consumption of these structures at level (4) is denoted R_g. Finally, at level (5), the total metabolic power consumption is denoted R_{tot}. It follows that the overall pump efficiency may be expressed as

$$\eta = P_p/R_{tot} = (P_p/P_{mek})(P_{mek}/R_p)(R_p/R_{tot}) = \eta_{mek}\eta_m(R_p/R_{tot}). \quad (38)$$

In many filter-feeders, it may be possible to measure, or indirectly estimate, the energy expenditure of the part of the body responsible for the pumping action (e.g. *Sabella penicillus* or *Mytilus edulis*); but in other animals it may be impossible (e.g *Nereis diversicolor*).

Thus, a 'standard' *Mytilus edulis* (shell length = 35 mm, gill area = 8·5 cm^2, beat frequency of lateral cilia = 10 Hz, filtration rate = 1 ml s^{-1}, pump head = 1 mm H_2O, useful pumping power = 10 μW, overall pump efficiency η = 1·1 %) has a total aerobic metabolic rate R_{tot} = 900 μW (Jørgensen *et al.*, 1986*a*) and a gill metabolic rate of R_g = 175 μW (Clemmesen & Jørgensen, 1987). The actual energy spent by the pump proper, the bands of lateral cilia and the cells carrying the cilia, is 34 % of the metabolic rate of the gill (Clemmesen & Jørgensen, 1987), i.e. $R_p = 175 \times 0{\cdot}34 = 59{\cdot}5$ μW,

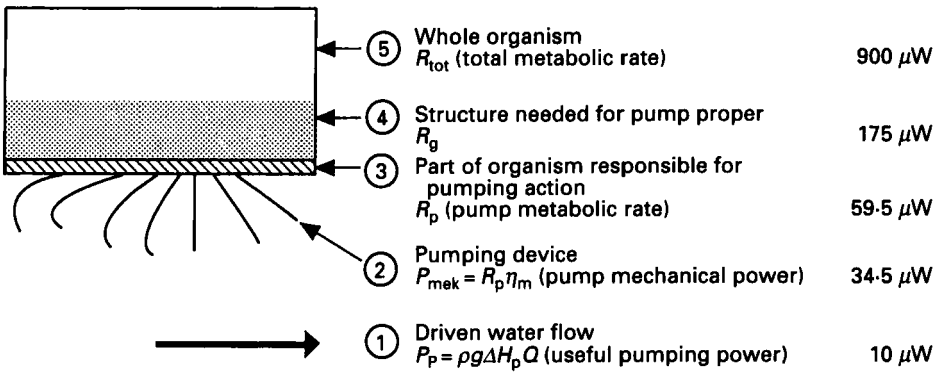

Fig. 14. Filter-feeding organism (schematic) with definitions of metabolic, mechanical, and pumping powers. Numerical values are estimates for *Mytilus edulis*.

resulting in $R_p/R_{tot} = 0{\cdot}066$. Clemmesen & Jørgensen (1987) estimated that the rate at which the active cilia hydrolyse ATP was 58 % of synthesis (at an ATP/dynein ratio of 2). This implies a metabolic to mechanical power conversion of $\eta_m = 0{\cdot}58$, hence $P_{mek} = 59{\cdot}5 \times 0{\cdot}58 = 34{\cdot}5\ \mu W$. By using equation (38), the mechanical efficiency of the bivalve pump may be estimated as $\eta_{mek} = 0{\cdot}011/(0{\cdot}58 \times 0{\cdot}066) = 0{\cdot}29$. Mechanical efficiencies of ciliated plane channel flow at various metachronisms, but at low amplitude ratios, have been calculated analytically by Nielsen & Larsen (1993), yielding values on the order of 0·1. Efficiencies of peristaltic motion in plane channels and tubes are given by Shapiro, Jaffrin & Weinberg (1969) and Takabatake, Ayukawa & Mori (1988). The numerical results of Takabatake *et al.* (1988) apply to large amplitude ratios, yielding $\eta_{mek} \approx 0{\cdot}3$–$0{\cdot}5$.

Referring to the powers estimated for *Mytilus edulis* in the foregoing example and listed at the five levels of Fig. 14, it may be argued that other measures of efficiency than the net pump efficiency (although it is the quantity most readily evaluated) may be appropriate when characterizing the energy cost of feeding of macro-invertebrates. Thus, a minimum efficiency would be $R_p/R_{tot} = 59{\cdot}5/900 = 6{\cdot}6\,\%$, rather than $\eta = P_p/R_{tot} = 10/900 = 1{\cdot}1\,\%$, since mechanical and metabolic energy conversion as well as the metabolism of cells carrying cilia must be included. Moreover, if the more realistic efficiency $R_g/R_{tot} = 175/900 = 19\,\%$ is used as a measure for energy cost it may be argued that the energetic costs of a filter-feeding bivalve with a large specialized gill-pump is not a negligible amount of the total metabolic rate. On the other hand, it can be argued that the high flow rate through the mantle cavity has rendered respiratory gills and oxygen transport via the blood, superfluous (Famme, 1981; Jørgensen *et al.* 1986*b*). Thus, it is not reasonable to question if filter-feeding is more expensive than surface-deposit-feeding for example. When considering the ratio $P_{mek}/R_g = 34{\cdot}5/175 = 20\,\%$ it is obvious that the water-transporting structures are expensive to maintain irrespective of whether the animal is pumping water or not. This supports the hypothesis that energy for functions other than pump work can only be justified when the part of the organism responsible for the pumping action is dimensioned for continuous feeding at low rates, rather than for discontinuous feeding at correspondingly higher rates (Jørgensen, 1975). Within the natural phytoplankton concentrations

found in the habitat, to which the filter-feeders are phylogenetically adapted, undisturbed animals are consistently observed to pump water continuously at rates characteristic for the species (e.g. Riisgård *et al.*, 1980; Riisgård & Randløv, 1981; Riisgård & Ivarsson, 1990; Riisgård 1991*a*, *b*; Vedel & Riisgård, 1993; Vedel *et al.*, 1994).

(2) *Temperature effects*

The acute effect of temperature on pumping rate has been studied in several ciliary filter-feeders. Thus, the mean increase in pumping rate of *Halichondria panicea* when the temperature was increased from 6 to 12 °C was $4{\cdot}3 \pm 2{\cdot}3$ times (Riisgård *et al.*, 1993). This increase may be compared to $2{\cdot}7 \pm 0{\cdot}3$ in *Ciona intestinalis* (Petersen & Riisgård, 1992, Table 2), $1{\cdot}4 \pm 0{\cdot}1$ in *Mytilus edulis* (Jørgensen *et al.*, 1990, Fig. 2), and $1{\cdot}2 \pm 0{\cdot}2$ times in *Sabella penicillus* (Riisgård & Ivarsson, 1990, equation (1), Fig. 6). Obviously there is no common temperature-dependent factor controlling the pumping rate in these ciliary filter-feeders. In *M. edulis* and *S. penicillus* the variation in pumping rate could be explained solely by the temperature-dependent changes in viscosity (Jørgensen *et al.*, 1990; Riisgård & Ivarsson, 1990); but not in *C. intestinalis* where a substantial effect of increased ciliary activity with temperature was suggested (Petersen & Riisgård, 1992). The very pronounced increase in *H. panicea* can not be explained by a combined effect of change in viscosity and change of beat frequency of the choanocyte flagella. The value of Q_{10} from equation (31) is usually between 2 and 3 for biological processes (including flagellar beat frequency). But, because the Q_{10} value for filtration rate in *H. panicea* varied between 4·2 and 25 (Riisgård *et al.*, 1993) the acute temperature effect in sponges may also be partly determined by factors such as constriction/dilation of inhalant canals and/or choanocyte chambers which may be temperature-dependent sites determining water flow.

Pump models including temperature effects has hitherto been used in the study of two filter-feeders. The models leading to equation (28) and (29) were proposed by Jørgensen *et al.* (1990) in the study of *Mytilus edulis*. The effect of temperature on the pump characteristic given by equation (28) was found to correspond to that expected for a ciliated channel (Nielsen & Larsen, 1993). For the closed pump of *Nereis diversicolor*, the effect of temperature on viscous leakage flow was modelled by Riisgård *et al.* (1992) using equation (26). It was found that the effects of viscosity were negligibly small in this type of positive displacement pump with limited viscosity dependent leakage and friction.

At present it may be concluded that the difficulties in the interpretation of observed results of pumping rates of filter-feeders at different temperatures are partly due to uncertainties related to proper acclimatization and partly due to possible couplings between biological and physical effects, e.g. through changes in morphological dimensions of pump and flow system. To separately study the physical effect of viscosity at constant temperature it may be proposed to increase the water viscosity by additives, e.g. biopolymers. While this has been useful in the study of beat frequency, forces and moments exerted by cilia or cirri on the fluid (Yoneda, 1960; Brokaw, 1966; Hiramoto, 1974) it has not yet been used with success to study pump-system behaviour.

(3) *Adaptation of pump- and filter-system to biotope*

The capacity for filtering water is the evolutionary result of the interplay between the organism and its environment, and the dimensioning of pump and filter-systems seems to be adapted to the phytoplankton concentrations prevailing in the biotope. This is illustrated by the following examples.

The maximal pressure rise and the normal operating pressure in the muscular-pumps of the polychaetes *Chaetopterus variopedatus* and *Nereis diversicolor* are nearly identical, but seem to be about twice as high as that in mussels, 4–5 times higher than that in ascidians and about 60 times higher than that in *Sabella penicillus* (Table 3). *C. variopedatus*, *N. diversicolor* and the ascidian *Styela clava* use a mucous net for trapping food particles, and it was suggested by Riisgård (1989) that the total mucous net area, the mesh size and the velocity of water through the net have been dimensioned in such a way as to make the resulting pressure drop a relatively low percentage (20–30%) of the maximal pressure rise which can be delivered by the pump. Thus, flow velocities through ascidian mucous nets which have been estimated at 0·3 mm s^{-1} in *S. clava* (Riisgård 1988*a*), 0·4 mm s^{-1} in *Ascidia mentula* (Jørgensen *et al.*, 1984) and 0·2 mm s^{-1} in *Ciona intestinalis* (Jørgensen, 1983). These rates can be compared to an estimated flow rate of 1·5 mm s^{-1} in *C. variopedatus* (Riisgård, 1989). The greater pressure rise, compared to ascidians, allows *C. variopedatus* to maintain higher flow velocity and thus to produce a mucous net which has one fifth of the area. The high pressure rise in *N. diversicolor* is not due to the mucous net because the velocity through the relatively large net is only 0·3 mm^{-1} (Riisgård *et al.*, 1992). The large net (with relatively large mesh) may be a compensation for an otherwise high system resistance in this facultatively filter-feeder in which filter-feeding may be presumed to be a relatively recent adaptation.

To assess the adaptation of a filter-feeding animal to the biotope it is of interest to know the rate of water transport in relation to the energy requirement of the animal. Thus, to obtain enough food to satiate the minimal energy requirements the performance of filter-feeders inhabiting inshore waters with high concentrations of phytoplankton must generally exceed 10 l of water per ml of oxygen consumed (Jørgensen, 1975). From this reference, the adaptation of filters-feeders to different phytoplankton concentrations may in this way be evaluated and compared (presuming similar particle retention efficiencies).

The water processing capacity of the 'standard' *Sabella penicillus* was estimated by Riisgård & Ivarsson, (1990) to be 354 l of water filtered per ml of oxygen consumed. This value may be compared to 50 l per ml of oxygen in *Chaetopterus variopedatus* (Riisgård, 1989). The seven times lower water processing capacity of *C. variopedatus*, which coexists with *S. penicillus*, may reflect different specialization in water processing and particle capturing efficiency. *C. variopedatus* retains particles down to about 1·5 μm with 100% efficiency with its mucous net, while the retention efficiency of the ciliary feeding *S. penicillus*, rapidly declines below 3 μm (Jørgensen *et al.*, 1984). The high water processing capacity of *S. penicillus* indicates that the animal is adapted to life in waters with extremely low algal concentrations. Throughout its ontogenetic development, the mussel *Mytilus edulis*, which retains particles down to 4 μm with 100% efficiency, processes 15–50 l water per ml of oxygen consumed (Riisgård *et al.*, 1980).

Table 3. *Normal operating pressure of pump* (ΔH_{op}), *power output* (P_{op}), *total metabolic rate of 'standard' animal* (R_{tot}) *and overall pump efficiency* ($\eta = P_{op}/R_{tot}$) *in different filter-feeding marine macro-invertebrates*

Taxonomic group and species	ΔH_{op} (mm H_2O)	P_{op} (μW)	R_{tot} (μW)	η (%)	References
Sponges					
Haliclona urceolus	0·673	0·677	80	0·85	Riisgård *et al.* (1993)
Bivalves					Jørgensen *et al.*
Mytilus edulis	1·0	10	900	1·1	(1986*a*, 1988)
Polychaetes					
Chaetopterus variopedatus	1·43	4·3	107	4·0	Riisgård (1989)
Nereis diversicolor	1·49	2·10	70	3·0	Riisgård *et al.*(1992)
Sabella penicillus	0·0224	0·451	112	0·403	Riisgård & Ivarsson (1990)
Ascidians					
Styela clava	0·3	2·3	891	0·26	Riisgård (1988*a*)

The coastal living *Nereis diversicolor* retains particles with about the same efficiency as *M. edulis* and it pumps about 40 l of water per ml oxygen consumed (Riisgård, 1991*a*). The two species seem to be adapted to similar regimes of suspended food particles. It may suggest that *M. edulis* and *N. diversicolor* are not able to live in the same localities as, for example, *S. penicillus* which seems to be a continuously water processing animal in which both the filter- and digestive systems are designed only to operate optimally at low phytoplankton concentrations (Riisgård & Ivarsson, 1990). A very different adaptation of filter and pump-system is found in sponges which only filter about 7 l of water per ml oxygen consumed (Riisgård *et al.*, 1993). The collar filter in sponges presumably retains particles with 100% efficiency down to 0·1 μm in diameter (Reiswig, 1971). This very high retention efficiency is in agreement with the lower filtration rates in sponges, though the biological significance of the high retention efficiency remains unknown at the present. It seems appropriate here to mention that thorough examinations of food particle size distributions and concentrations of most filter-feeder biotopes still awaits execution. Of particular interest is the mean concentration and composition of suspended particles (bacteria, phytoplankton, silt etc.) in the inhalant water actually filtered by the animals which may experience different degrees of a particle-depleted boundary layer due to e.g. strong intraspecific competition and inefficient mixing in stagnant water (see e.g. Riisgård, 1994; O'Riordan, Monismith & Koseff, 1993).

VII. CONCLUSIONS

Filter-feeding marine macro-invertebrates must filter large volumes of water to meet their food requirements, and therefore the energy cost of water pumping has been a debated subject. During recent years a number of filter-feeding animals (sponges, polychaetes, bivalves and ascidians) have been characterized by means of engineering principles and analysis of the energetics of biological pumps.

For each filter-feeder, it is possible to identify a pump and a system. The pump drives water at a certain flow rate against various resistances to flow in the system, such as canals, filters etc. If the pressure head delivered by the pump versus volume flow, i.e.

the pump characteristic, and the head loss due to the resistance to flow in the system, i.e. the system characteristic, are plotted in the same graph then the intersection of the two characteristics defines the operating point (determining the resulting flow and pressure head) of the pump-system arrangement. In the species examined in the present review, the system characteristic was expressed as the sum of viscous resistance, kinetic head loss and externally imposed back pressure. The first two contributions were estimated by using standard equations for head losses and detailed morphological data on the geometry of the flow system. Further, the back-pressure pumping-rate characteristic was experimentally determined. This information determines indirectly the pump-characteristic and thus the operating pump pressure. Separate considerations of pump modelling serve to characterize the pump and test the consistency of the results.

Because the useful power received by the water equals the product of the pump pressure and volume flow rate, the power output of the different filter-pumps could be determined and related to the total metabolic power expenditure (estimated from the respiration rate). For representatives of the various taxonomic groups examined, such results show that the useful pump work constitutes from 0·3 to 4% of the total metabolic expenditure. Filter-feeding in marine environments is based on the evolution of low-energy pumps that continuously process the surrounding water through filters dimensioned to the phytoplankton concentrations of the biotope.

VIII. ACKNOWLEDGEMENTS

Thanks are due to Prof. C. Barker Jørgensen, Dr. Cliff Warman and Dr. Gary Banta for critical remarks and suggestions for improving the style of the manuscript. We thank an anonymous referee for valuable comments and suggestions which substantially improved the paper.

IX. REFERENCES

BAYNE, B. L., THOMPSON, R. & WIDDOWS, J. (1976). Physiology (I). In *Marine Mussels: Their Ecology and Physiology* (ed. B. L. Bayne), pp. 121–206. Cambridge University Press, Cambridge.

BERGQUIST, P. R. (1978). *Sponges*. University of California, Berkeley and Los Angeles.

BERNARD, F. R. & NOAKES, D. J. (1990). Pumping rates, water pressures, and oxygen use in eight species of marine bivalve molluscs from British Columbia. *Canadian Journal of Fisheries and Aquatic Sciences* **47**, 1302–1306.

BIDDER, G. P. (1923). The relation of the form of a sponge to its currents. *Quarterly Journal of Microscopical Science* **67**, 293–323.

BROKAW, C. J. (1966). Effects of increased viscosity on the movements of some invertebrate spermotozoa. *Journal of Experimental Biology* **45**, 113–139.

BROWN, S. C. (1975). Biomechanics of water-pumping by *Chaetopterus variopedatus* Renier. Skeletomusculature and kinematics. *Biological Bulletin. Marine Biological Laboratory, Woods Hole, MA* **149**, 136–150.

BROWN, S. C. (1977). Biomechanics of water-pumping by *Chaetopterus variopedatus* Renier: kinetics and hydrodynamics. *Biological Bulletin. Marine Biological Laboratory, Woods Hole, MA* **153**, 121–132.

CHAPMAN, G. (1968). The hydraulic system of *Urechis caupo* Fisher & MacGinitie. *Journal of Experimental Biology* **49**, 657–667.

CLEMMESEN, B. & JØRGENSEN, C. B. (1987). Energetic costs and efficiencies of ciliary filter feeding. *Marine Biology* **94**, 445–449.

CONOVER, R. J. (1968). Zooplankton – life in a nutritionally dilute environment. *American Zoologist* **8**, 107–118.

COUGHLAN, J. (1969). The estimation of filtering from the clearance of suspensions. *Marine Biology* **2**, 356–358.

EVANS, S. M. (1971). Behaviour in polychaetes. *Quarterly Review of Biology* **46**, 379–405.

FAMME, P. (1981). Haemolymph circulation as a respiratory parameter in the mussel *Mytilus edulis* L. *Comparative Biochemistry and Physiology* **69A**, 243–247.

FAMME, P., RIISGÅRD, H. U. & JØRGENSEN, C. B. (1986). On direct measurements of pumping rates in the mussel *Mytilus edulis*. *Marine Biology* **92**, 323–327.

FIALA-MÉDIONI, A. (1978). A scanning electron microscope study of the branchial sac of benthic filter-feeding invertebrates (Ascidians). *Acta Zoologica, Stockholm* **59**, 1–9.

FJERDINGSTAD, E. J. (1961*a*). The ultrastructure of choanocyte collars in *Spongilla lacustris* (L.). *Zeitschrift für Zellforschung and Microskopische Anatomie* **53**, 645–57.

FJERDINGSTAD, E. J. (1961*b*). Ultrastructure of the collar of the choanoflagellate *Codonosiga botrytis* (Ehrenb.). *Zeitschrift für Zellforschung und Microskopische Anatomie* **54**, 499–510.

FLOOD, P. R. & FIALA-MÉDIONI, A. (1981). Ultrastructure and histochemistry of the branchial sac of benthic filter-feeding invertebrates (Ascidians). *Acta Zoologica, Stockholm* **59**, 1–9.

FLOOD, P. R. & FIALA-MÉDIONI, A. (1982). Structure of the mucous feeding filter of *Chaetopterus variopedatus* (Polychaeta). *Marine Biology* **72**, 27–33.

FOSTER-SMITH, R. L. (1976*a*). Pressures generated by the pumping mechanism of some ciliary filter-feeders. *Journal of Experimental Marine Biology and Ecology* **25**, 199–206.

FOSTER-SMITH, R. L. (1976*b*). Some mechanisms for the control of pumping activity in bivalves. *Marine Behaviour and Physiology* **4**, 41–60.

FOSTER-SMITH, R. L. (1978). An analysis of water flow in tube-living animals. *Journal of Experimental Marine Biology and Ecology* **34**, 73–95.

FOX, R. W. & MCDONALD, A. T. (1985). *Introduction to Fluid Mechanics*. John Wiley & Sons, New York.

FROST, T. M. (1978). In situ measurements of clearance rates for the freshwater sponge *Spongilla lacustris*. *Limnology and Oceanography* **23**, 1034–1039.

GARBY, L. & LARSEN, P. S. (1994). *Bioenergetics, its Thermodynamic Foundations*. Cambridge University Press, Cambridge. (in press).

GALTSOFF, P. S. (1926). New methods to measure the rate of flow produced by the gills of oysters and other mollusca. *Science* Washington D.C. **63**, 233–234.

GOERKE, H. (1966). Nahrungsfiltration von *Nereis diversicolor* O. F. Müller (Nereidae, Polychaeta). *Veröffentlichungen des Institut für Meersforschung in Bremerhaven* **10**, 49–58.

HAPPEL, J. & BRENNER, H. (1965). *Low Reynolds Number Hydrodynamics*. Prentice-Hall, Inc., Englewood Cliffs, NJ.

HARLEY, M. M. (1950). Occurrence of a filter-feeding mechanism in the polychaete *Nereis diversicolor*. *Nature, London* **165**, 734–735.

HIBBERD, D. J. (1975). Observations on the ultrastructure of the choanoflagellate *Codosiga botrytis* (Ehr.) Saville-Kent with special reference to the flagellar apparatus. *Journal of Cell Science* **17**, 191–219.

HIRAMOTO, Y. (1974). Mechanisms of cilia movement, In *Cilia and Flagella* (ed M. A. Sleigh), pp. 177–198 Academic Press, London.

HOLLEY, M. C. (1986). Cell shape, spatial patterns of cilia, and mucus-net construction in the ascidian endostyle. *Tissue & Cell* **18**, 667–684.

JONES, H. D. & ALLEN, J. R. (1986). Inhalant and exhalant pressures in *Mytilus edulis* and *Cerastoderma edule*. *Journal of Experiment Marine Biology and Ecology* **98**, 231–240.

JØRGENSEN, C. B. (1966). *Biology of Suspension Feeding*. Pergamon Press, Oxford.

JØRGENSEN, C. B. (1975). Comparative physiology of suspension feeding. *Annual Review of Physiology* **37**, 57–79.

JØRGENSEN, C. B. (1983). Fluid mechanical aspects of suspension feeding. *Marine Ecology – Progress Series* **11**, 89–103.

JØRGENSEN, C. B., KIØRBOE, T., MØHLENBERG, F. & RIISGÅRD, H. U. (1984). Ciliary and mucus net filter feeding, with special reference to fluid mechanical characteristics. *Marine Ecology – Progress Series* **15**, 283–292.

JØRGENSEN, C. B., FAMME, P., SAUSTRUP KRISTENSEN, H., LARSEN, P. S., MØHLENBERG, F. & RIISGÅRD, H. U. (1986*a*). The bivalve pump. *Marine Ecology – Progress Series* **34**, 69–77.

JØRGENSEN, C. B., MØHLENBERG, F. & STEN-KNUDSEN, O. (1986*b*). Nature of relation between ventilation and oxygen consumption in filter feeders. *Marine Ecology – Progress Series* **29**, 73–88.

JØRGENSEN, C. B. & RIISGÅRD, H. U. (1988). Gill pump characteristics of the soft clam *Mya arenaria*. *Marine Biology* **99**, 107–109.

JØRGENSEN, C. B., LARSEN, P. S., MØHLENBERG, M. & RIISGÅRD, H. U. (1988). The bivalve pump: properties and modelling. *Marine Ecology – Progress Series* **45**, 205–216.

JØRGENSEN, C. B. (1989). Water processing in ciliary feeders with special reference to the bivalve filter pump. *Comparative Biochemistry and Physiology* **94**, 383–394.

JØRGENSEN, C. B. (1990). *Bivalve Filter Feeding: Hydrodynamics, Bioenergetics, Physiology and Ecology*. Olsen & Olsen, Fredensborg, Denmark.

JØRGENSEN, C. B., LARSEN, P. S. & RIISGÅRD, H. U. (1990). Effects of temperature on the mussel pump. *Marine Ecology – Progress Series* **64**, 89–97.

JØRGENSEN, C. B. (1992). Adaptational, environmental, and ecological physiology. A case for hierachical thinking. In *Physiological Adaptations in Vertebrates, Respiration, Circulation and Metabolism*. (Ed S. C. Wood, R. E. Weber, A. R. Hargens and R. W. Millard), pp. 9–17. Marcel Dekker, Inc., New York, Basel, Hong Kong.

LaBarbera, M. & Vogel, S. (1976). An inexpensive thermistor flowmeter for aquatic biology. *Limnology and Oceanography* **21**, 750–756.

LaBarbera, M. (1990). Principles of design of fluid transport systems in zoology. *Science* **249**, 992–1000.

Larsen, P. S. & Riisgård, H. U. (1994). The sponge pump. *Journal of Theoretical Biology* **168**, 53–63.

Laval, M. (1971). Ultrastructure et mode de nutrition du choanoflagellé *Salpingoeca pelagica*, sp.nov. Comparaison avec les choanocytes des spongiaires. *Protistologica* **7**, 325–336.

Leyton, L. (1975). *Fluid behaviour in Biological Systems*. Clarendon Press, Oxford.

MacGinitie, G. E. (1939). The method of feeding of *Chaetopterus*. *Biological Bulletin. Marine Biological Laboratory, Woods Hole, MA* **77**, 115–118.

Marks, L. S. (ed.) (1941). *Mechanical Engineers' Handbook*. McGraw-Hill Book Company, Inc., New York.

Mayer, S. (1994). Particle capture in the crown of the ciliary suspension feeding polychaete *Sabella penicillus*: Videotape recordings and interpretations. *Marine Biology* **119**, 571–582.

McNeill Alexander, R. (1975). *The Chordates*. Cambridge University Press. Cambridge.

Meyhöfer, E. (1985). Comparative pumping rates in suspension-feeding bivalves. *Marine Biology* **85**, 137–142.

Millar, R. H. (1971). The biology of ascidians. *Advanced Marine Biology* **9**, 1–100.

Munson, B. R. (1988). Very low Reynolds number flow through screens. *Journal of Fluids Engineering* **110**, 462–463.

Møhlenberg, F. & Riisgård, H. U. (1978). Efficiency of particle retention in 13 species of suspension feeding bivalves. *Ophelia* **17**, 239–246.

Møhlenberg, F. & Riisgård, H. U. (1979). Filtration rate, using a new indirect technique, in thirteen species of suspension-feeding bivalves. *Marine Biology* **54**, 143–148.

Nicol, E. A. T. (1931). The feeding mechanism, formation of the tube and physiology of digestion in *Sabella pavonia*. *Transaction of the Royal Society, Edinburgh* **56**, 537–597.

Nielsen, C. (1987). Structure and function of metazoan ciliary bands and their phylogenetic significance. *Acta Zoologica, Stockholm* **68**, 202–262.

Nielsen, N. F., Larsen, P. S., Riisgård, H. U. & Jørgensen, C. B. (1993). Fluid motion and particle retention in the gill of *Mytilus edulis*: video recordings and numerical modelling. *Marine Biology* **116**, 61–71.

Nielsen, N. F. & Larsen, P. S. (1993). A note on ciliated channel flow with a pressure gradient. *Journal of Fluid Mechanics* **257**, 97–110.

Owen, G. & McCrae, J. M. (1976). Further studies on the latero-frontal tracts of bivalves. *Proceedings of the Royal Society, London, Series B*, **194**, 527–544.

O'Riordan, C. A., Monismith, S. G. & Koseff, J. R. (1993). A study of concentration boundary layer formation over a bed of model bivalves. *Limnology and Oceanography* **38**, 1712–1729.

Orrhage, L. (1980). On the structure and homologues of the anterior end of the polychaete families sabellidae and serpulidae. Zoomorphology **96**, 113–168.

Petersen, J. K. & Riisgård, H. U. (1992). Filtration capacity of the ascidian *Ciona intestinalis* (L.) and its grazing impact in a shallow fjord. *Marine Ecology – Progress Series* **88**, 9–17.

Randløv, A. & Riisgård, H. U. (1979). Efficiency of particle retention and filtration rate in four species of ascidians. *Marine Ecology – Progress Series* **1**, 55–59.

Rawson, K. J. & Tupper, E. C. (1968). *Basic Ship Theory*. American Elsevier, New York.

Reiswig, H. M. (1971). Particle feeding in natural populations of three marine demosponges. *Biological Bulletin* **141**, 568–591.

Reiswig, H. M. (1975). The aquiferous systems of three marine demospongiae. *Journal of Morphology* **145**, 493–502.

Riisgård, H. U. (1977). On measurements of the filtration rates of suspension feeding bivalves in a flow system. *Ophelia* **16**, 167–173.

Riisgård, H. U. & Møhlenberg, F. (1979). An improved automatic recording apparatus for determining the filtration rate of *Mytilus edulis* as a function of size and algal concentration. *Marine Biology* **52**, 61–67.

Riisgård, H. U., Randløv, A. & Sand Kristensen, P. (1980). Rates of water processing oxygen consumption and efficiency of particle retention in veligers and young post-metamorphic *Mytilus edulis*. Ophelia **19**, 37–47.

Riisgård, H. U. & Randløv, A. (1981). Energy budgets, growth and filtration rates in *Mytilus edulis* at different algal concentration. *Marine Biology* **61**, 227–234.

Riisgård, H. U. (1988*a*). The ascidian pump: properties and energy cost. *Marine Ecology – Progress Series* **47**, 129–134.

Riisgård, H. U. (1988*b*). Efficiency of particle retention and filtration rate in 6 species of Northeast American bivalves. *Marine Ecology – Progress Series* **45**, 217–223.

Riisgård, H. U. (1989). Properties and energy cost of the muscular piston pump in the suspension feeding polychaete *Chaetopterus variopedatus*. *Marine Ecology – Progress Series* **56**, 157–168.

RIISGÅRD, H. U. & IVARSSON, N. M. (1990). The crown-filament-pump of the suspension-feeding polychaete *Sabella penicillus*: filtration, effects of temperature, energy cost, and modelling. *Marine Ecology – Progress Series* **62**, 249–257.

RIISGÅRD, H. U. (1991*a*). Suspension feeding in the polychaete *Nereis diversicolor*. *Marine Ecology – Progress Series* **70**, 29–37.

RIISGÅRD, H. U. (1991*b*). Filtration rate and growth in the blue mussel, *Mytilus edulis* Linneaus, 1758: dependence on algal concentration. *Journal of Shellfish Research* **10**, 29–35.

RIISGÅRD, H. U., VEDEL, A., BOYE, H. & LARSEN, P. S. (1992). Filter-net structure and pumping activity in the polychaete *Nereis diversicolor*: effects of temperature and pump-modelling. *Marine Ecology – Progress Series* **83**, 79–89.

RIISGÅRD, H. U., THOMASSEN, S., JAKOBSEN, H., WEEKS, J. M. & LARSEN, P. S. (1993). Suspension feeding in marine sponges *Halichondria panicea* and *Haliclona urceolus*: effects of temperature on filtration rate and energy cost of pumping. *Marine Ecology – Progress Series* **96**, 177–188.

RIISGÅRD, H. U. (1994). Filter-feeding in the polychaete *Nereis diversicolor*: A review. *Netherlands Journal of Aquatic Ecology* **28**, (In the press).

SHAPIRO, A. H., JAFFRIN, M. Y. & WEINBERG, S. L. (1969). Peristaltic pumping with long wavelengths at low Reynolds number. *Journal Fluid Mechanics* **37**, 799–825.

SHIMETA, J. S. & JUMARS, P. A. (1991). Physical mechanisms and rates of particle capture by suspension feeders. *Oceanography and Marine Biology, an Annual Review* **29**, 191–257.

SILVESTER, N. R. (1983). Some hydrodynamic aspects of filter feeding with rectangular-mesh nets. *Journal of Theoretical Biology* **103**, 265–286.

SIMPSON, T. L. (1984). *The Cell Biology of Sponges*. Springer-Verlag, New York, Berlin, Heidelberg, Tokyo.

TAKABATAKE, S., AYUKAWA, K. & MORI, A. (1988). Peristaltic pumping in circular cylindrical tubes: a numerical study of fluid transport and its efficiency. *Journal of Fluid Mechanics* **193**, 267–283.

TAMADA, K. & FUJIKAWA, H. (1957). The steady two-dimensional flow of viscous fluid at low Reynolds numbers passing through an infinite row of equal parallel circular cylinders. *Quarterly Journal of Mechanics and Applied Mathematics* **10**, 426–432.

VAHL, O. (1973). Porosity of the gill, oxygen consumption and pumping rate in *Cardium edule* (L.) (Bivalvia). *Ophelia* **10**, 109–118.

VEDEL, A. & RIISGÅRD, H. U. (1993). Filter-feeding in the polychaete *Nereis diversicolor*: growth and bioenergetics. *Marine Ecology – Progress Series* **100**, 145–152.

VEDEL, A., ANDERSEN, B. B. & RIISGÅRD, H. U. (1994). Field investigations of pumping activity of the facultatively filter-feeding polychaete *Nereis diversicolor* using an improved infrared phototransducer system. *Marine Ecology – Progress Series* **103**, 91–101.

VERDUIN, J. (1969). Hard clam pumping rates: Energy requirements. Science **166**, 1309–1310.

VOGEL, S. (1981). *Life in Moving Fluids. The Physical Biology of flow*. Princeton University Press, New Jersey.

WALSHAW, A. C. & JOBSON, D. A. (1979). *Mechanics of Fluids*, 3rd edn. Longman, London.

WELLS, G. P. & DALES, R. P. (1951). Spontaneous activity patterns in animal behaviour: the irrigation of the burrow in the polychaetes *Chaetopterus variopedatus* Renier and *Nereis diversicolor* O. F. Müller. *Journal of the Marine Biology Association of the United Kingdom* **29**, 661–680.

WHITE, F. M. (1974). *Viscous Fluid Flow*. McGraw-Hill Inc., New York.

YONEDA, M. (1960). Force exerted by a single cilium of *Mytilus edulis* I. *Journal of Experimental Biology* **37**, 461–468.